RESEARCH ARTICLE SUMMARY

YEAST GENETICS

A global genetic interaction network maps a wiring diagram of cellular function

Michael Costanzo,* Benjamin VanderSluis,* Elizabeth N. Koch,* Anastasia Baryshnikova,* Carles Pons,* Guihong Tan,* Wen Wang, Matej Usaj, Julia Hanchard, Susan D. Lee, Vicent Pelechano, Erin B. Styles, Maximilian Billmann, Jolanda van Leeuwen, Nydia van Dyk, Zhen-Yuan Lin, Elena Kuzmin, Justin Nelson, Jeff S. Piotrowski, Tharan Srikumar, Sondra Bahr, Yiqun Chen, Raamesh Deshpande, Christoph F. Kurat, Sheena C. Li, Zhijian Li, Mojca Mattiazzi Usaj, Hiroki Okada, Natasha Pascoe, Bryan-Joseph San Luis, Sara Sharifpoor, Emira Shuteriqi, Scott W. Simpkins, Jamie Snider, Harsha Garadi Suresh, Yizhao Tan, Hongwei Zhu, Noel Malod-Dognin, Vuk Janjic, Natasa Przulj, Olga G. Troyanskaya, Igor Stagljar, Tian Xia, Yoshikazu Ohya, Anne-Claude Gingras, Brian Raught, Michael Boutros, Lars M. Steinmetz, Claire L. Moore, Adam P. Rosebrock, Amy A. Caudy, Chad L. Myers,† Brenda Andrews,† Charles Boone†

INTRODUCTION: Genetic interactions occur when mutations in two or more genes combine to generate an unexpected phenotype. An extreme negative or synthetic lethal genetic interaction occurs when two mutations, neither lethal individually, combine to cause cell death. Conversely, positive genetic interactions occur when two mutations produce a phenotype that is less severe than expected. Genetic interactions identify functional relationships between genes and can be harnessed for biological discovery and therapeutic target identification. They may also explain a considerable component of the undiscovered genetics associated with human diseases. Here, we describe construction and analysis of a comprehensive genetic interaction network for a eukaryotic cell.

RATIONALE: Genome sequencing projects are providing an unprecedented view of genetic variation. However, our ability to interpret genetic information to predict inherited phenotypes remains limited, in large part due to the extensive buffering of genomes, making most individual eukaryotic genes dispensable for life. To explore the extent to which genetic interactions reveal cellular function and contribute to complex phenotypes, and to discover the general principles of genetic networks, we used automated yeast genetics to construct a global genetic interaction network.

RESULTS: We tested most of the ~6000 genes in the yeast *Saccharomyces cerevisiae* for all possible pairwise genetic interactions, identifying nearly 1 million interactions, including ~550,000 negative and ~350,000 positive interactions, spanning ~90% of all yeast genes. Essential genes were network hubs, displaying five times as many interactions as nonessential genes. The set of genetic interactions or the genetic interaction profile for a gene provides a quantitative measure of function, and a global network based on genetic interaction profile similarity revealed a hierarchy of modules reflecting the functional architecture of a cell. Negative interactions connected functionally related genes, mapped core bioprocesses, and identified pleiotropic genes, whereas positive interactions often mapped general regulatory connections associated with defects in cell cycle progression or cellular proteostasis. Importantly, the global network illustrates how coherent sets of negative or positive genetic interactions connect protein complex and pathways to map a functional wiring diagram of the cell.

ON OUR WEBSITE

Read the full article at http://dx.doi.org/10.1126/science.aaf1420

CONCLUSION: A global genetic interaction network highlights the functional organization of a cell and provides a resource for predicting gene and pathway function. This network emphasizes the prevalence of genetic interactions and their potential to compound phenotypes associated with single mutations. Negative genetic interactions tend to connect functionally related genes and thus may be predicted using alternative functional information. Although less functionally informative, positive interactions may provide insights into general mechanisms of genetic suppression or resiliency. We anticipate that the ordered topology of the global genetic network, in which genetic interactions connect coherently within and between protein complexes and pathways, may be exploited to decipher genotype-to-phenotype relationships. ■

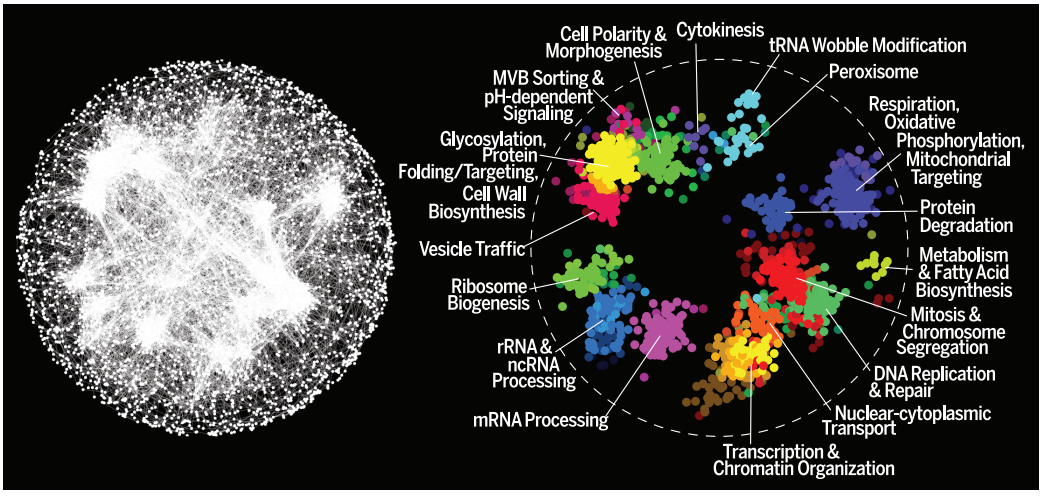

A global network of genetic interaction profile similarities. (**Left**) Genes with similar genetic interaction profiles are connected in a global network, such that genes exhibiting more similar profiles are located closer to each other, whereas genes with less similar profiles are positioned farther apart. (**Right**) Spatial analysis of functional enrichment was used to identify and color network regions enriched for similar Gene Ontology bioprocess terms.

The list of author affiliations is available in the full article online.
*These authors contributed equally to this work.
†Corresponding author. Email: cmyers@cs.umn.edu (C.L.M.); brenda.andrews@utoronto.ca (B.A.); charlie.boone@utoronto.ca (C.B.)
Cite this article as M. Costanzo *et al.*, *Science* **353**, aaf1420 (2016). DOI: 10.1126/science.aaf1420

RESEARCH ARTICLE

YEAST GENETICS

A global genetic interaction network maps a wiring diagram of cellular function

Michael Costanzo,[1*] Benjamin VanderSluis,[2,3*] Elizabeth N. Koch,[2*] Anastasia Baryshnikova,[4*] Carles Pons,[2*†] Guihong Tan,[1*] Wen Wang,[2] Matej Usaj,[1] Julia Hanchard,[1,5] Susan D. Lee,[6] Vicent Pelechano,[7‡] Erin B. Styles,[1,5] Maximilian Billmann,[8] Jolanda van Leeuwen,[1] Nydia van Dyk,[1] Zhen-Yuan Lin,[9] Elena Kuzmin,[1,5] Justin Nelson,[2,10] Jeff S. Piotrowski,[1,11§] Tharan Srikumar,[12||] Sondra Bahr,[1] Yiqun Chen,[1] Raamesh Deshpande,[2] Christoph F. Kurat,[1¶] Sheena C. Li,[1,11] Zhijian Li,[1] Mojca Mattiazzi Usaj,[1] Hiroki Okada,[13] Natasha Pascoe,[1,5] Bryan-Joseph San Luis,[1] Sara Sharifpoor,[1] Emira Shuteriqi,[1] Scott W. Simpkins,[2,10] Jamie Snider,[1] Harsha Garadi Suresh,[1] Yizhao Tan,[1] Hongwei Zhu,[1] Noel Malod-Dognin,[14] Vuk Janjic,[15] Natasa Przulj,[14,16] Olga G. Troyanskaya,[3,4] Igor Stagljar,[1,5,17] Tian Xia,[2,18] Yoshikazu Ohya,[13] Anne-Claude Gingras,[5,9] Brian Raught,[12] Michael Boutros,[8] Lars M. Steinmetz,[7,19] Claire L. Moore,[6] Adam P. Rosebrock,[1,5] Amy A. Caudy,[1,5] Chad L. Myers,[2,10#] Brenda Andrews,[1,5#] Charles Boone[1,5,11#]

We generated a global genetic interaction network for *Saccharomyces cerevisiae*, constructing more than 23 million double mutants, identifying about 550,000 negative and about 350,000 positive genetic interactions. This comprehensive network maps genetic interactions for essential gene pairs, highlighting essential genes as densely connected hubs. Genetic interaction profiles enabled assembly of a hierarchical model of cell function, including modules corresponding to protein complexes and pathways, biological processes, and cellular compartments. Negative interactions connected functionally related genes, mapped core bioprocesses, and identified pleiotropic genes, whereas positive interactions often mapped general regulatory connections among gene pairs, rather than shared functionality. The global network illustrates how coherent sets of genetic interactions connect protein complex and pathway modules to map a functional wiring diagram of the cell.

Genetic interaction networks highlight mechanistic connections between genes and their corresponding pathways (*1*). Genetic interactions can also determine the relationship between genotype and phenotype (*2*) and may contribute to the "missing heritability," or the lack of identified genetic determinants underlying a phenotypic trait, in current genome-wide association studies (*3*, *4*). To explore the general principles of genetic networks, we took a systematic approach to map genetic interactions among gene pairs in the budding yeast, *Saccharomyces cerevisiae*. Synthetic genetic array (SGA) analysis automates the combinatorial construction of defined mutants and enables the quantitative analysis of genetic interactions (*1*, *5*). A positive genetic interaction describes a double mutant that exhibits a fitness that is greater than expected based on the combination of the two corresponding single mutants. Conversely, a negative or synthetic lethal/sick genetic interaction is identified when a double mutant displays a fitness defect that is more extreme than expected (*1*, *5*). Synthetic lethal interactions are of particular interest because they can be harnessed to identify new antibiotic or cancer therapeutic targets (*6*, *7*). In this study, we both expand upon our previous analysis of genetic interactions associated with nonessential genes (*1*) and also characterize genetic interactions involving the majority of essential genes to generate a global yeast genetic interaction network.

A global and quantitative genetic network for yeast

To map genetic interactions between nonessential yeast genes (*8*), we generated a genome-scale library of *natMX*-marked deletion mutant query strains and crossed them to an array composed of the corresponding *kanMX*-marked deletion mutant collection (*9*, *10*). We also systematically examined genetic interactions between pairs of essential genes (*9*, *10*). To do so, we generated temperature-sensitive (TS) mutant alleles, carrying mutations that typically alter coding regions. Our essential gene mutant collection consists of 2001 array and/or query strains harboring TS alleles corresponding to 868 unique essential genes, with ~600 of these genes represented by two or more TS alleles, including strains for ~140 essential genes that were not represented in previous strain collections (*11*, *12*). TS mutants were screened at a semipermissive temperature where cells were viable but partially compromised for gene function and associated with a reduced growth rate (*8*). We also constructed a set of essential gene query strains carrying decreased abundance of mRNA (DAmP) alleles, which can lead to reduced transcript levels (*13*); however, only a fraction of DAmP alleles (25%) compromised gene function enough to affect cellular fitness (>5% fitness defect) and, consequently, most DAmP alleles exhibited fewer interactions compared with TS alleles of essential genes (fig. S1). Thus, TS alleles mediated the majority of the essential gene genetic interactions in our network, and the analyses described exclude DAmP alleles, unless otherwise noted.

We constructed three different genetic interaction maps. First, the collection of nonessential deletion mutant query strains was screened against the nonessential deletion mutant array

[1]The Donnelly Centre, University of Toronto, 160 College Street, Toronto ON, Canada M5S 3E1. [2]Department of Computer Science and Engineering, University of Minnesota-Twin Cities, 200 Union Street, Minneapolis, MN 55455, USA. [3]Simons Center for Data Analysis, Simons Foundation, 160 Fifth Avenue, New York, NY 10010, USA. [4]Lewis-Sigler Institute for Integrative Genomics, Princeton University, Princeton, NJ 08544, USA. [5]Department of Molecular Genetics, University of Toronto, 160 College Street, Toronto ON, Canada M5S 3E1. [6]Department of Developmental, Molecular and Chemical Biology, Tufts University School of Medicine, Boston, MA 02111, USA. [7]European Molecular Biology Laboratory (EMBL), Genome Biology Unit, 69117 Heidelberg, Germany. [8]Division of Signaling and Functional Genomics, German Cancer Research Center (DKFZ) and Heidelberg University, Heidelberg, Germany. [9]Lunenfeld-Tanenbaum Research Institute, Mount Sinai Hospital, Toronto ON, Canada. [10]Program in Biomedical Informatics and Computational Biology, University of Minnesota–Twin Cities, 200 Union Street, Minneapolis, MN 55455, USA. [11]Chemical Genomics Research Group, RIKEN Center for Sustainable Resource Sciences (CSRS), Saitama, Japan. [12]Princess Margaret Cancer Centre, University Health Network and Department of Medical Biophysics, University of Toronto, Toronto ON, Canada. [13]Department of Integrated Biosciences, Graduate School of Frontier Sciences, University of Tokyo, Kashiwa, Chiba, Japan 277-8561. [14]Computer Science Department, University College London, London WC1E 6BT, UK. [15]Department of Computing, Imperial College London, UK. [16]School of Computing (RAF), Union University, Belgrade, Serbia. [17]Department of Biochemistry, University of Toronto, Toronto, ON, Canada. [18]School of Electronic Information and Communications, Huazhong University of Science and Technology, Wuhan, China, 430074. [19]Department of Genetics, School of Medicine and Stanford Genome Technology Center Stanford University, Palo Alto, CA 94304, USA.
*These authors contributed equally to this work. †Present address: Institute for Research in Biomedicine (IRB Barcelona), The Barcelona Institute for Science and Technology, Barcelona, Catalonia, Spain. ‡Present address: Science for Life Laboratory, Department of Microbiology, Tumor and Cell Biology. Karolinska Institutet, Solna, Sweden. §Present address: Yumanity Therapeutics, 790 Memorial Drive, Cambridge, MA 02139, USA. ||Present address: Department. of Molecular Biology, Princeton University, Princeton, NJ, USA. ¶Present address: The Francis Crick Institute, Clare Hall Laboratory, South Mimms, Herts. EN6 3LD, UK. **#Corresponding author. Email: cmyers@cs.umn.edu (C.L.M.); brenda.andrews@utoronto.ca (B.A.); charlie.boone@utoronto.ca (C.B.)**

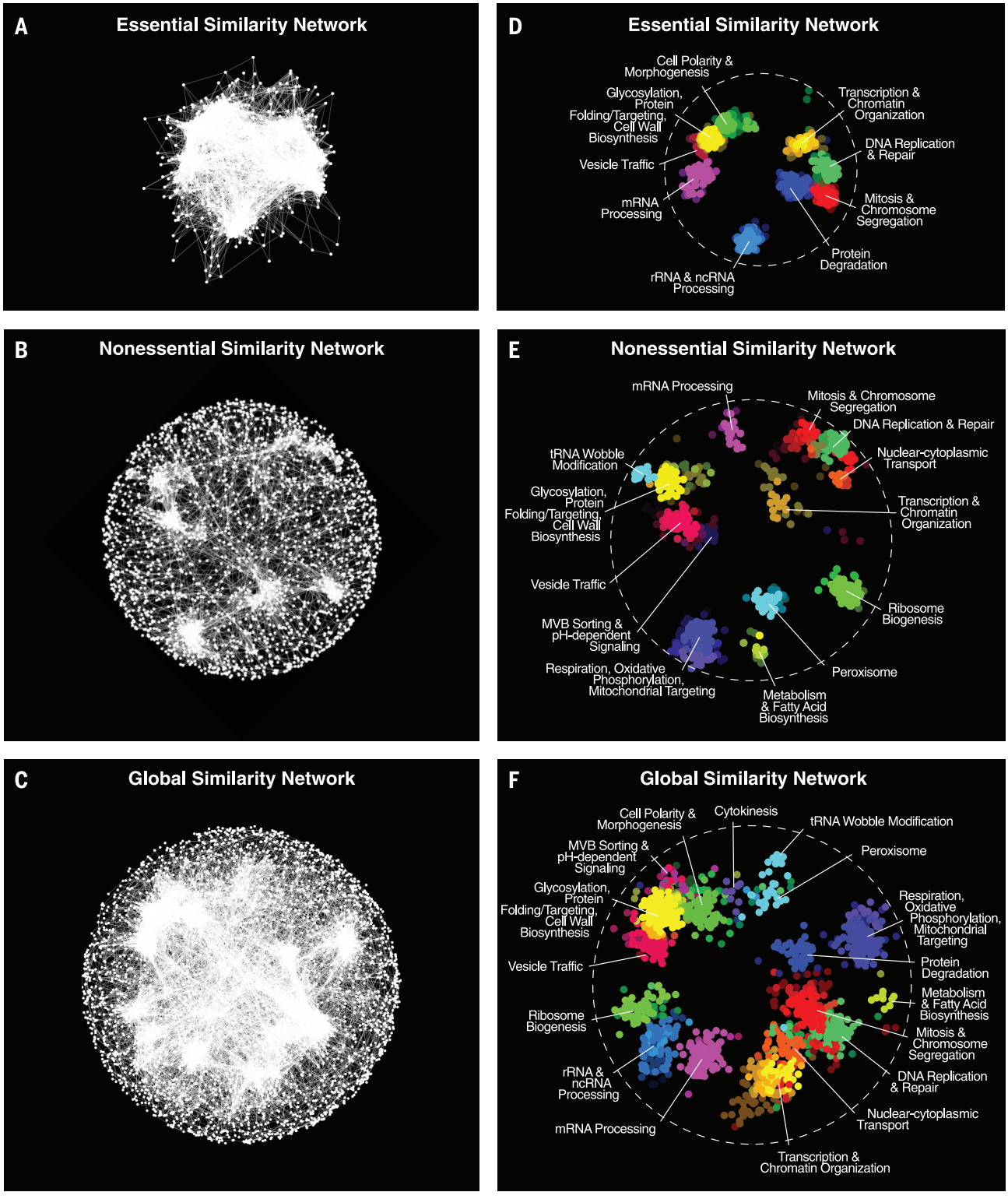

Fig. 1. A global network of genetic interaction profile similarities. (**A**) The essential similarity network was constructed by computing PCCs for genetic interaction profiles (edges) of all pairs of genes (nodes) in the essential genetic interaction matrix (ExE). Gene pairs with profile similarity of PCC > 0.2 were connected and graphed using a spring-embedded layout algorithm. Genes sharing similar genetic interaction profiles map proximal to each other, whereas genes with less similar genetic interaction profiles are positioned farther apart. (**B**) A genetic profile similarity network for the nonessential genetic interaction matrix (NxN). (**C**) A global genetic profile similarity network encompassing all nonessential and essential genes was constructed from the combined NxN, ExE, and NxE genetic interaction matrices. (**D**) The essential similarity network was annotated using SAFE, identifying network regions enriched for similar GO biological process terms, which are color-coded. (**E**) The nonessential similarity network annotated using SAFE. (**F**) The global similarity network annotated using SAFE.

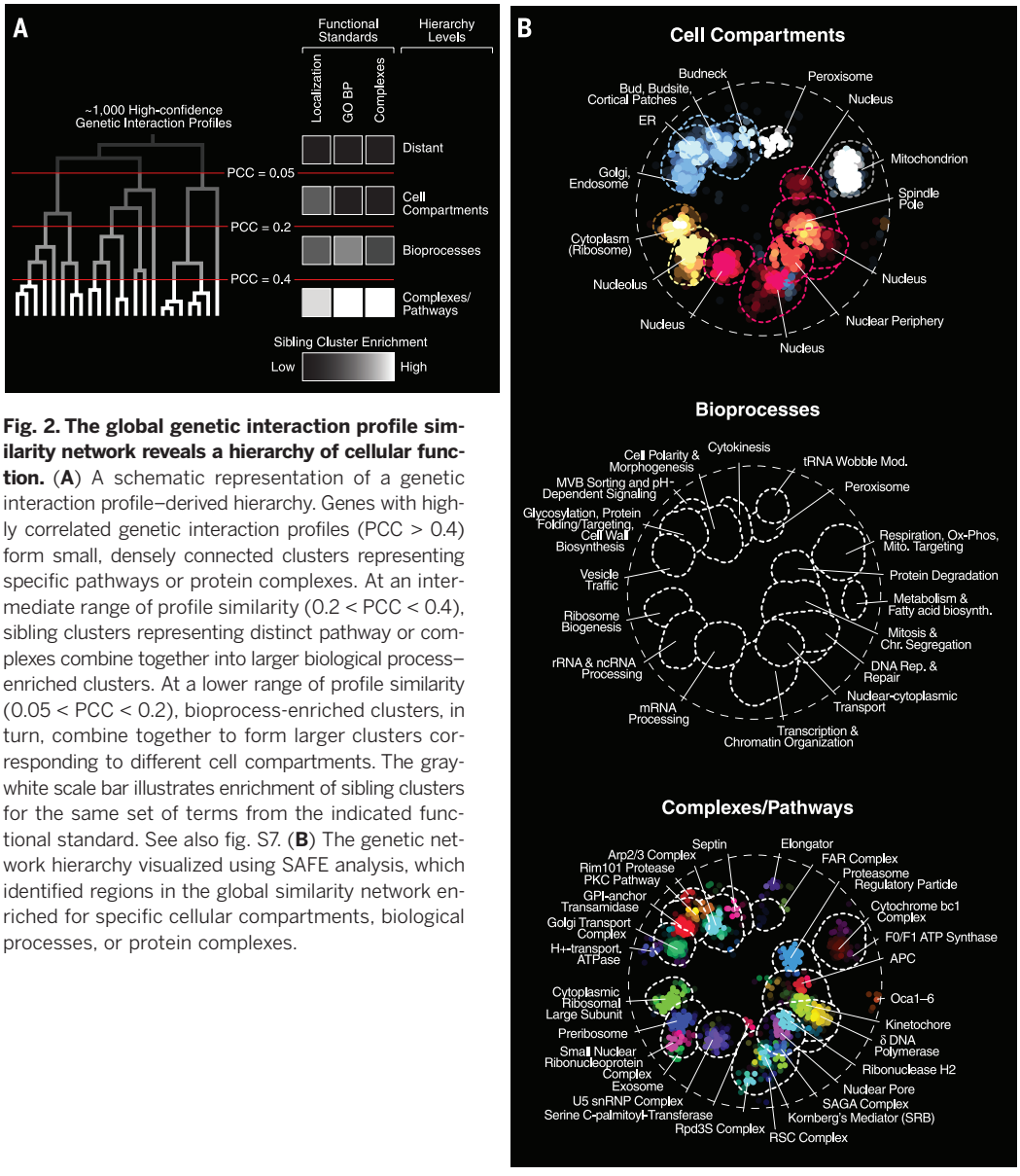

Fig. 2. The global genetic interaction profile similarity network reveals a hierarchy of cellular function. (**A**) A schematic representation of a genetic interaction profile–derived hierarchy. Genes with highly correlated genetic interaction profiles (PCC > 0.4) form small, densely connected clusters representing specific pathways or protein complexes. At an intermediate range of profile similarity (0.2 < PCC < 0.4), sibling clusters representing distinct pathway or complexes combine together into larger biological process–enriched clusters. At a lower range of profile similarity (0.05 < PCC < 0.2), bioprocess-enriched clusters, in turn, combine together to form larger clusters corresponding to different cell compartments. The gray-white scale bar illustrates enrichment of sibling clusters for the same set of terms from the indicated functional standard. See also fig. S7. (**B**) The genetic network hierarchy visualized using SAFE analysis, which identified regions in the global similarity network enriched for specific cellular compartments, biological processes, or protein complexes.

to generate a nonessential x nonessential (NxN) network. Second, query strains carrying TS alleles of essential genes were also screened against the nonessential deletion mutant array to generate an essential x nonessential (ExN) network. Finally, both nonessential deletion mutant and TS query mutant strains were crossed to an array of TS strains of essential genes to generate an expanded ExN network and the first large-scale essential x essential (ExE) genetic network.

Negative and positive genetic interactions were quantified and false negative/positive rates and data reproducibility were determined at defined confidence thresholds (*1*) from analysis of biological replicates and comparison of interactions for a subset of gene pairs represented on both mutant arrays (fig. S2) (*8*). A global genetic interaction network resulting from the combination of the NxN, ExN, and ExE networks was generated from analysis of ~23 million double mutants encompassing 5416 different genes. In total, we identified nearly 1 million genetic interactions, corresponding to ~550,000 negative and ~350,000 positive genetic interactions, including ~120,000 interactions between pairs of essential genes (fig. S3). The current global network involves ~90% of all yeast genes as query and/or array mutants and is accessible from http://thecellmap.org/costanzo2016/. The experiments and analyses described here were from a representative subset (>80%) of the complete data set (data files S1 to S3).

A functional map of a cell

The genetic interaction profile of a particular gene is composed of its specific set of negative and positive genetic interactions. Genes belonging to similar biological processes tend to share common genetic interactions, and genes encoding proteins that function together within the same pathway or complex display similar genetic interaction profiles (fig. S4) (*1*). Thus, genetic interaction profiles provide a quantitative measurement of functional similarity, and similarity networks generated from the correlation of large-scale genetic interaction profiles organize genes into clusters that highlight biological processes (*1*). We visualized networks of genetic profile similarity (data file S3) between essential genes (Fig. 1A), nonessential genes (Fig. 1B), and a combined global similarity network (Fig. 1C). Nodes in the similarity networks represent genes, whereas edges connect gene pairs that share similar genetic interaction profiles (*8*).

When evaluated at the same Pearson correlation coefficient (PCC) threshold, the essential gene similarity network (Fig. 1A) was more than 25-fold more densely connected compared with the corresponding nonessential network (Fig. 1B). For example, at PCC ≥ 0.2, 3.12% of all tested gene pairs were connected in the ExE similarity network, whereas 0.12% of all tested gene pairs were connected in the NxN similarity network. Moreover, genes on the essential gene similarity network often showed a stronger functional relationship, because genes that encode members of the same essential protein complex exhibited significantly higher interaction profile similarity than gene pairs belonging to the same nonessential complex (fig. S5). By evaluating the predictive power of both essential and nonessential genetic interaction profiles (*8*), we found that essential gene interaction profiles provided higher-accuracy gene function predictions across a diverse set of different Gene Ontology (GO) biological processes (*14*), and this increased accuracy was correlated with the fraction of essential genes annotated to specific bioprocesses (fig. S6 and data file S4). Nevertheless, interactions involving either essential or nonessential genes can predict function. For example, interactions involving nonessential genes were more predictive of vacuolar transport, peroxisome, and mitochondrial function, whereas interactions involving essential genes were more informative for predicting chromosome segregation, mRNA splicing, and proteolysis functions. Interestingly, functional predictions for essential genes could also be derived from interactions with nonessential genes and vice versa. Nevertheless, optimal functional prediction performance was achieved with a global similarity network that combined the majority of all nonessential and

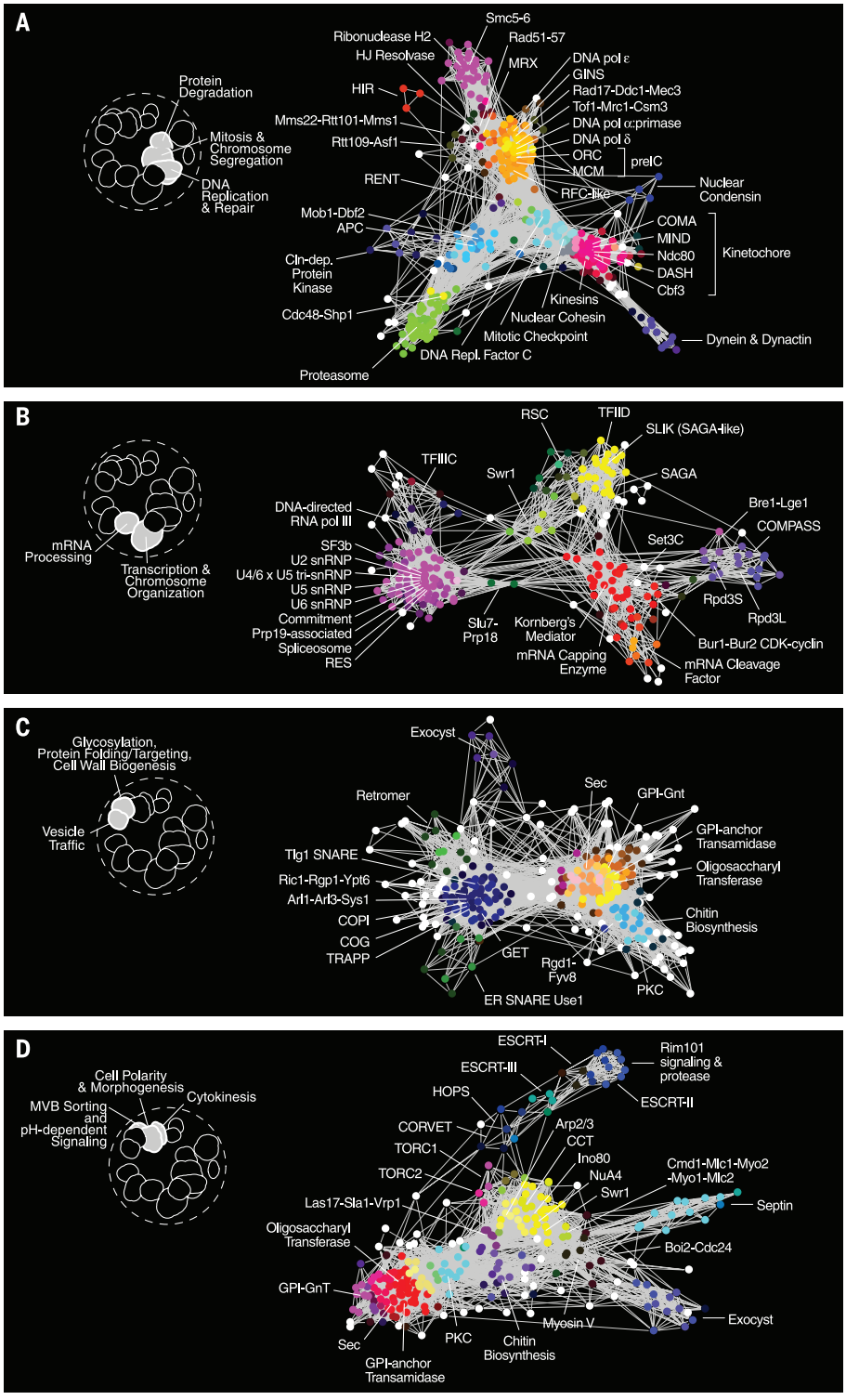

Fig. 3. Genetic interaction profile similarity subnetworks. Genes belonging to the indicated biological process–enriched clusters were extracted from the global network and laid out using a spring-embedded layout algorithm. Subnetworks were annotated using SAFE to identify network regions enriched for specific protein complexes. (**A**) Protein complexes localized within the protein degradation, mitosis and chromosome segregation, and DNA replication and repair, enriched bioprocess clusters shown in Fig. 1F. (**B**) Protein complexes localized within the transcription and chromatin organization and mRNA processing-enriched bioprocess clusters shown in Fig. 1F. (**C**) Protein complexes localized within the glycosylation, protein folding/targeting, cell wall biosynthesis, and vesicle traffic–enriched bioprocess clusters shown in Fig. 1F. (**D**) Protein complexes localized within the multivesicular body (MVB) sorting and pH-dependent signaling, cell polarity and morphogenesis, and cytokinesis-enriched bioprocess clusters shown in Fig. 1F.

essential protein coding genes in the *S. cerevisiae* genome.

To functionally annotate the global genetic profile similarity maps (Fig. 1, A to C), we applied spatial analysis of functional enrichment (SAFE), which identifies dense network regions associated with specific functional attributes (*15*). Implementing SAFE with 4373 biological process terms from Gene Ontology (GO) (*14*), we detected gene clusters in each similarity network that were enriched for unique sets of related GO terms (Fig. 1, D to F, and data file S5). Gene clusters enriched for GO terms related to cell polarity, protein degradation, and ribosomal RNA (rRNA) processing were specifically detected in the essential gene similarity network (Fig. 1D), whereas the nonessential gene similarity network identified clusters enriched for mitochondrial and peroxisomal functions (Fig. 1E). The global similarity network provided a more organized and functionally comprehensive view of cellular function, emphasizing the importance of mapping genetic interactions that involve both nonessential and essential genes (Fig. 1F). SAFE identified 487 significantly enriched GO bioprocess terms that mapped to 17 unique network regions and covered 1343 genes on the global network (Fig. 1F). The subsets of enriched GO bioprocess terms associated with each densely connected network region in turn revealed genes involved in core cellular functions and defined an informative subset of GO bioprocess terms associated with these functions (data file S5).

Genetic profile similarities map a hierarchy of gene and cellular function

The relative positioning of biological process clusters appeared to reflect shared functionality because distinct, but related, processes—such as DNA replication and repair and mitosis and chromosome segregation—were positioned next to each other in the global similarity network (Fig. 1F). To explore this functional organization more rigorously, we considered only those genes with at least one highly similar gene partner, resulting in a set of 515 nonessential and 421 essential array mutants (*8*). We then applied an unsupervised clustering approach to construct a genetic interaction–based hierarchy for this subset of genes. The base of the resultant hierarchy was composed of numerous, small clusters of genes with highly similar genetic interaction profiles, whereas the top of the hierarchy was composed of a small set of larger clusters of genes with lower profile similarity (Fig. 2A, fig. S7, and data file S6).

To examine functional relationships between clusters identified at different hierarchical levels, we assessed whether distinct "sibling" clusters, resolved at one level of the hierarchy and combined together at a higher level to generate a unique and larger "parent" cluster, shared enrichment for the same annotations from a particular functional standard (*8*). Indeed, sibling clusters identified at a relatively high level of profile similarity (e.g., PCC > 0.4), which often corresponded to distinct protein complexes, shared enrichment for the same GO biological

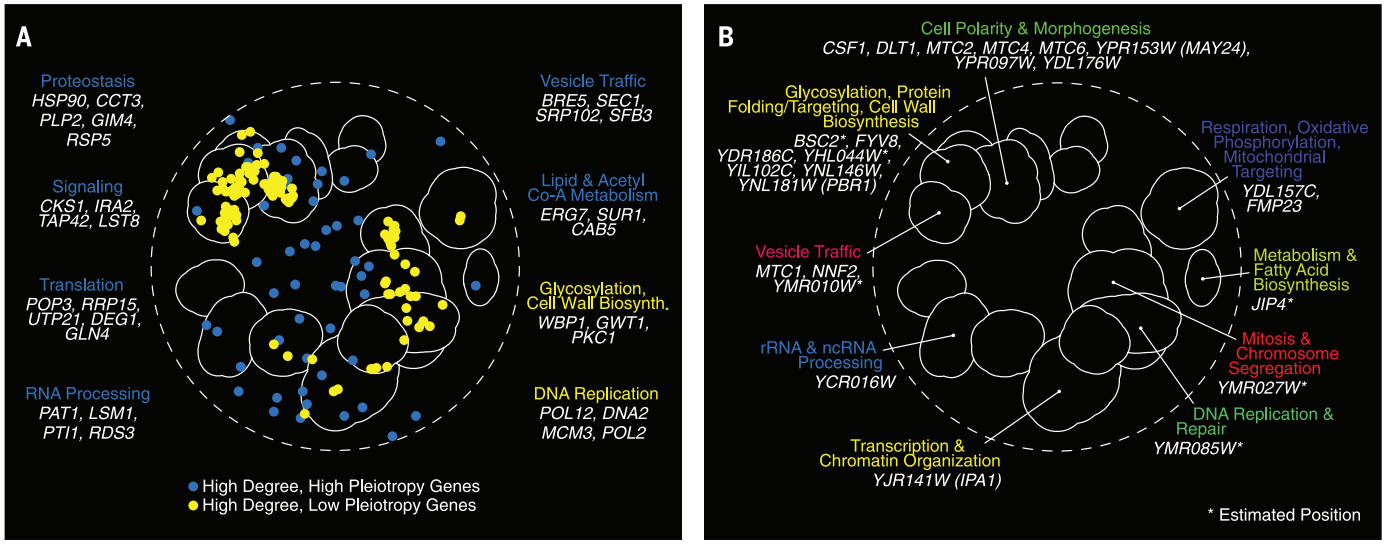

Fig. 4. Using network connectivity to explore gene function. (**A**) Highly connected hub genes identified either as pleiotropic (blue nodes), or functionally specific (yellow nodes), are highlighted on a schematic representation of the global similarity network. Examples of high (blue text) and low (yellow text) pleiotropy genes, grouped based on their general function, are shown. (**B**) Poorly characterized genes that localize within, or in the vicinity of, a specific biological process–enriched cluster on the global similarity network. An estimated network position is indicated (*) for genes that are not present on the global similarity network because their genetic interaction profile similarity to other genes does not exceed a PCC > 0.2. Network position for these genes was estimated as described (*8*).

process annotations (data file S6). For example, five sibling clusters with distinct pathway/complex annotations, including the homologous DNA repair pathway and the ORC (origin recognition complex), combined together into a single parent cluster, and all these siblings are enriched for GO biological process terms such as "DNA repair," "DNA metabolic process," and "response to DNA damage stimulus," which reflects a general role shared by the collective gene set in the regulation of DNA synthesis and repair (data file S6).

However, sibling clusters detected at an intermediate range of profile similarity (0.2 < PCC < 0.4), which combined into a relatively smaller set of larger parent clusters at a lower range of profile similarity (0.05 < PCC < 0.2), did not share enrichment for the same GO biological process, pathways, or protein complex annotations. Instead, these clusters were enriched for genes whose products function in the same cell compartment (Fig. 2A, fig. S7, and data file S6). For example, one of the 10 parent clusters formed near the top of the hierarchy was composed of six sibling clusters, and, although each individual sibling cluster was enriched for unique GO biological process terms including "chromosome segregation," "transcription from RNA polymerase II promoter," or "DNA repair," none of the sibling clusters were enriched for the same GO biological process terms. Instead, all 10 sibling clusters were enriched for gene products that exhibit nuclear localization patterns (data file S6). As observed previously (*16*), this indicates that novel functional organization is embedded within large-scale, unbiased data sets, which may not be captured completely by functional standards, including GO as it is currently organized (*14*). Thus, a global genetic interaction network, created on the basis of a single fitness phenotype, quantifies functional relatedness to organize genes into modules corresponding to protein complexes and pathways, which combine to define specific biological processes. These biological processes, in turn, group together into larger modules representing specific cellular compartments, thereby revealing a hierarchical model of cell function.

The functional hierarchy revealed by genetic interaction profiles can also be visualized on the global similarity network (Fig. 2B). Applying SAFE with a protein localization standard (*17*), we detected 14 network regions enriched for genes whose products localize to 11 different subcellular compartments (Fig. 2B, Cell Compartments). For example, bioprocess clusters such as DNA replication and repair, mitosis and chromosome segregation, nuclear-cytoplasmic transport, and transcription and chromatin organization (Fig. 2B, Bioprocesses and data file S5) combined into a single module encompassing genes localized to the cell nucleus (Fig. 2B, Cell Compartments). At a higher level of functional resolution, SAFE identified 28 gene clusters corresponding to 123 specific protein complexes (Fig. 2B, Complexes/Pathways and data file S5). Functional relationships between protein complexes were also resolved in greater detail by extracting biological process-enriched clusters from the global network and visualizing them in isolation (Fig. 3 and data file S5).

Quantifying genetic pleiotropy

The ability of an organism to tolerate environmental and genetic variation may be dependent on phenotypic capacitors, a class of genes whose inactivation may increase phenotypic variation among genetically diverse individuals in a population (*18*). Hsp90, the canonical capacitor, is a molecular chaperone controlling numerous signaling pathways and thus is considered a multifunctional or pleiotropic gene (*18*). Identifying other pleiotropic genes may uncover novel capacitors and provide insight into the genetic basis of phenotypic robustness.

We expect that a pleiotropic gene involved in diverse functions should show a genetic interaction profile that partially overlaps with genes representative of its functional spectrum. To quantify pleiotropy, we focused on genes with a high degree of negative genetic interactions and developed a pleiotropy score that measured the functional breadth of genetic interaction profiles associated with these genes (*8*). Genes encoding Hsp90 (*hsc82Δ hsp82-5001* TS double-mutant query strain) (data file S1); *IRA2*, a negative regulator of RAS signaling; and *RSP5*, an E3 ubiquitin ligase, ranked among the most highly pleiotropic genes observed (data file S7). Other highly pleiotropic genes (top 30% pleiotropy scores) included those with proteostasis or signaling roles, as well as select genes with roles in fundamental cellular functions, such as translation, RNA processing, vesicle trafficking, lipid and acetyl Co-A metabolism (Fig. 4A). Because they share genetic interactions with many functionally diverse genes, high pleiotropy genes were often positioned outside the functionally enriched clusters, scattered in the sparser regions of the global network (Fig. 4A). In contrast, high-degree but low-pleiotropy genes (lowest 30% pleiotropy scores), which are functionally specific, were positioned more frequently in densely connected regions of the global similarity network ($P < 10^{-5}$; Gene Set Enrichment Analysis) (*8*).

Predicting novel gene function

The location of numerous previously uncharacterized genes, either within or in close proximity to

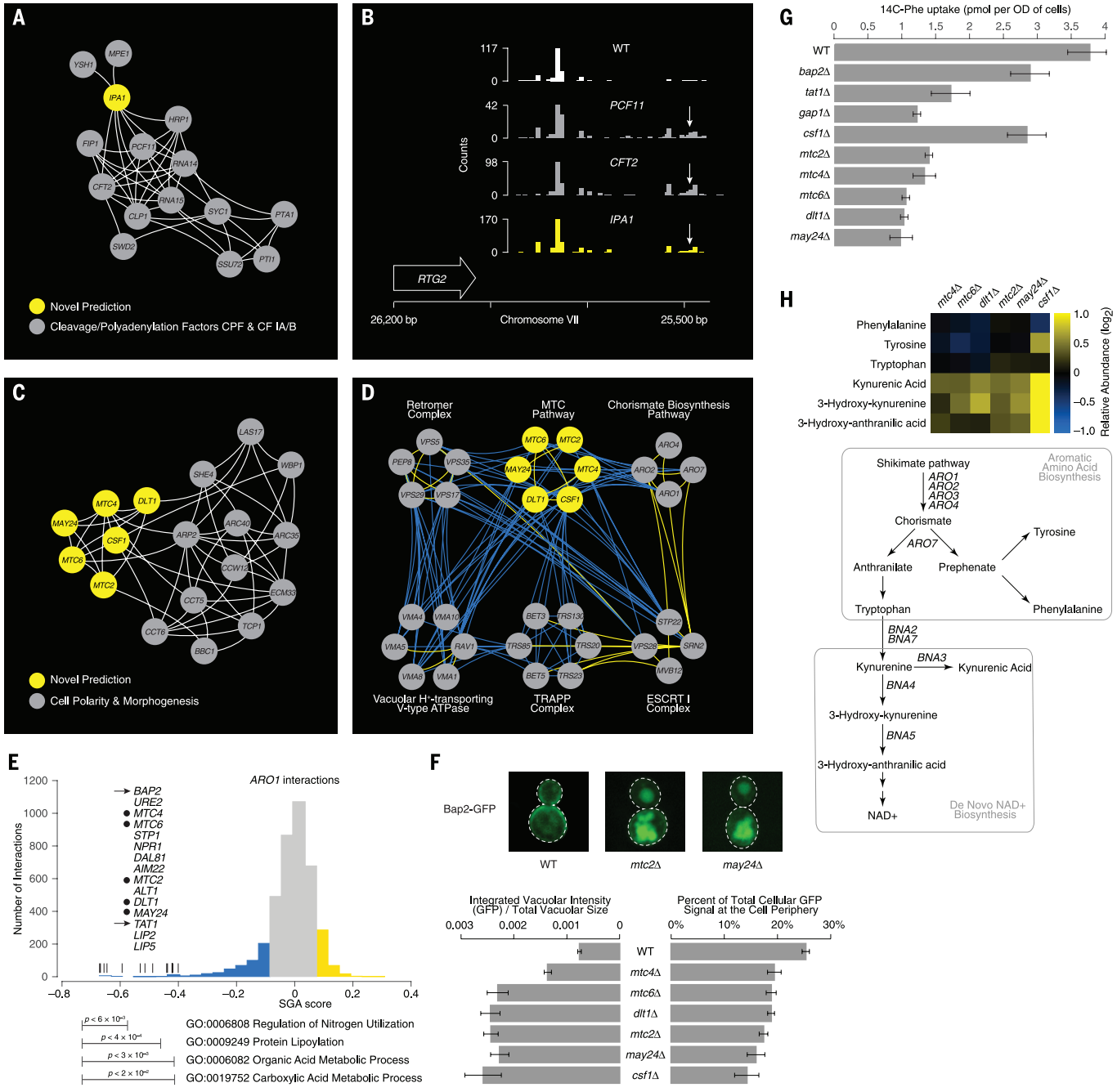

Fig. 5. Validating functional predictions for IPA1 and the MTC pathway. (**A**) A genetic interaction profile similarity subnetwork for the uncharacterized essential gene, *IPA1* (yellow node), extracted from the transcription and chromatin organization enriched biological process cluster. (**B**) Polyadenylation profiles for a representative gene, *RTG2*, generated from genome-wide sequencing of mRNA purified from a wild-type (WT) strain and strains carrying TS mutations of *PCF11*, *CFT2*, or *IPA1*. The horizontal arrow indicates the orientation of the *RTG2* open reading frame; the vertical arrows indicate the mutant, increased aberrant, 3′ mRNA cleavage and polyadenylation. (**C**) A genetic interaction profile similarity subnetwork for *MTC2*, *MTC4*, *MTC6*, *CSF1*, *DLT1*, and *MAY24* genes (yellow nodes) extracted from the network region in the vicinity of the cell polarity and morphogenesis biological process cluster. (**D**) The MTC pathway genetic interaction network. Nodes are grouped according to genetic interaction profile similarity and edges represent negative (blue) and positive (yellow) interactions (genetic interaction score, $|\varepsilon| > 0.08$, $P < 0.05$). (**E**) Distribution of *ARO1* negative (blue) and positive (yellow) genetic interactions ($|\varepsilon| > 0.08$, $P < 0.05$) (gene pairs that failed to meet the threshold for interactions are colored gray). Functions enriched among genes that displayed an extreme negative interaction with *ARO1* are indicated, and a subset of these genes and where they are located within the SGA score distribution is shown. Closed circles indicate members of the MTC pathway, and arrows indicate amino acid permease encoding genes. (**F**) (Top) Representative cell images illustrating Bap2-GFP (green fluorescent protein) localization in WT, *mtc2*Δ, and *may24*Δ deletion mutant strains. (Bottom) Vacuolar intensity (total GFP signal in the vacuole/vacuolar area) and percentage of total cellular GFP present at the cell periphery (cell periphery GFP/total cellular GFP signal) were quantified for WT cells and MTC pathway mutants. Error bars indicate standard deviation from three replicate experiments. (**J**) Cellular uptake of ^{14}C-labeled phenylalanine in WT and deletion mutant strains. Error bars indicate standard deviation from three replicate experiments. (**H**) (Top) Metabolite levels for the indicated mutants were analyzed by full-scan liquid chromatography–mass spectrometry. The levels of selected metabolites are presented as $\log_2$ ratios relative to wild type cells. (Bottom) Schematic diagram illustrating aromatic amino acid and de novo NAD$^+$ biosynthesis pathways.

functionally enriched regions of the genetic profile similarity network, allows us to predict functions for these genes (Fig. 4B) (*8*). Notably, while most essential genes are relatively well studied, our network uncovered a role for a previously uncharacterized essential gene, *YJR141W*, which we named *IPA1* (important for cleavage and polyadenylation), in the highly conserved process of mRNA 3′-end processing and polyadenylation. *IPA1* shares many genetic interactions in common with genes encoding members of the cleavage/polyadenylation factor (CPF) and cleavage factor IA (CF IA) protein complexes (Figs. 4B and 5A), which, along with *HRP1*, are essential for mRNA 3′ end processing (*19*). We also found that Ipa1 physically interacted with CPF complex members Mpe1 and Ysh1 (data file S8) (*8*), further supporting a role for *IPA1* in this process. Indeed, as shown previously for TS mutants in components of CF IA and CPF complexes (*20*), such as *pcf11* and *cft2* TS mutants, an *ipa1* TS mutant was impaired for in vitro mRNA cleavage and polyadenylation (fig. S8) and showed widespread defects in mRNA processing accuracy and efficiency, with a significant bias toward the use of downstream polyadenylation sites ($P < 2 \times 10^{-16}$; Wilcoxon rank sum) (Fig. 5B and fig. S8) (*8*).

Six poorly characterized genes—*MTC2*, *MTC4*, *MTC6*, *CSF1*, *DLT1*, and *YPR153W*—localized in the vicinity of the cell polarity and morphogenesis cluster on the global network (Fig. 4B) and displayed highly similar genetic interaction profiles, suggesting that they work together as a novel functional module (Fig. 5C). Interestingly, all of these genes were identified as important for growth in high-pressure and cold environments (*21*). Thus, we called this module the MTC pathway and named *YPR153W* as *MAY24* (genetic interaction profile similarity to MTC annotated yeast genes *MTC2* and *MTC4*). *MTC2*, *MTC4*, and *MTC6* mutants were previously shown to enhance the mutant phenotype associated with perturbation of *CDC13*, which controls the maintenance of telomere capping (*22*). We found that the MTC pathway genes showed strong negative interactions with protein-trafficking genes, as well as aromatic amino acid biosynthesis genes *ARO1* and *ARO2* (Fig. 5D and fig. S9). Because pathway components often share phenotypes with their target genes, a genetic interaction profile that contains members of a particular pathway may also identify potential targets of the same pathway. For example, the *ARO1* genetic interaction profile revealed strong negative interactions with genes involved in amino acid metabolism, the entire MTC pathway, and the aromatic amino acid transporters *BAP2* and *TAT1* (Fig. 5E and fig. S9), suggesting that the MTC pathway may control amino acid metabolism or affect trafficking of Bap2 and Tat1 permeases. Indeed, mutations of MTC pathway genes resulted in Bap2 mislocalization (Fig. 5F and fig. S9) and a defect in phenylalanine uptake, resembling that of strains deleted for genes encoding amino acid transporters, including *BAP2*, *TAT1*, and *GAP1* (Fig. 5G) (*8*). Furthermore, unbiased metabolomics analysis revealed that the MTC pathway mutants exhibited elevated levels of kynurenine biosynthetic pathway metabolites, precursors of nicotinamide adenine dinucleotide (oxidized form) (NAD^+) (Fig. 5H) (*8*). Previous studies showed that defects in kynurenine biosynthesis suppressed *cdc13-1* TS mutants, suggesting that elevated NAD^+ levels inhibit telomere capping (*23*). Thus, the global genetic interaction network traced functional connections whereby defects in MTC pathway-dependent protein trafficking alter aromatic amino acid homeostasis, which appears to modulate steady-state levels of kynurenine biosynthetic pathway metabolites, linking cell polarity to telomere capping through altered NAD^+ levels.

Genetic interaction network connectivity

Genetic interaction profiles connect a particular gene to other genes through both negative and positive interactions. Although the average gene participated in ~100 negative interactions (2% of genes tested) and ~65 positive interactions (1% of genes tested), when assessed at an intermediate confidence threshold (*8*), a wide range of connectivity exists in the genetic interaction network (fig. S10 and data file S9). For example, the 10% most connected genes (i.e., high interaction degree genes or hub genes) in the genetic interaction network participated in 3.5-fold more genetic interactions than the average gene. More specifically, negative interaction hubs had an average degree of 340 negative interactions, and the average positive interaction hub displayed 200 positive interactions. In general, essential genes participated in ~5-fold more negative and positive interactions than nonessential genes, confirming previous estimates (Fig. 6A) (*24*).

As observed previously (*1*), fitness defects associated with both deletion alleles of nonessential genes and TS alleles of essential genes were highly correlated with the degree of genetic interaction (figs. S11 and S12, table S1, and data file S10). In the global network, genetic interaction hubs tended to encode conserved, multifunctional, highly expressed, and abundant proteins that exhibit many physical interactions and also participated in numerous chemical-genetic interactions (data file S9 and table S1). Genes encoding proteins involved in specific biochemical functions, or those that contain specific functional domains, such as an SH3 (SRC homology 3) protein-protein interaction domain, were also associated with a higher number of genetic interactions (figs. S13 and S14). In the nonessential genetic interaction network (NxN), negative and positive interaction hubs were enriched for biological processes including chromatin organization, transcription, and vesicle trafficking (data file S11). In the essential genetic network (ExE), negative interaction hubs were relatively uniformly distributed across all bioprocesses, whereas positive interaction hubs were specifically enriched for proteostasis-related bioprocesses (data file S11).

Genes that exhibited relatively few genetic interactions were also associated with specific features (figs. S11 to S14, table S2, and data file S10). For example, ATP-binding cassette transporters, which belong to functionally redundant gene families and thus are extensively buffered, exhibited fewer genetic interactions (figs. S11 to S14 and table S2). Interestingly, genes with the lowest interaction degree (lowest 20%) (data file S9) were often associated with more deleterious single-nucleotide polymorphisms (SNPs), exhibited a higher ratio of nonsynonymous to synonymous nucleotide substitutions (dN/dS), and displayed high expression variance across different genetic backgrounds and environments. This suggests that these genes are under reduced evolutionary constraints and subject to condition-specific regulation (table S2 and figs. S11 and S12). About 1000 genes (~20%), the majority of which are nonessential genes, displayed few genetic interactions and had profiles that generally displayed a relatively low level of functional information, suggesting that the connectivity for some genes will only be revealed under different environmental or genetic conditions. The functional, physiological, and evolutionary properties associated with genetic interaction frequency should predict genetic network connectivity and candidate genes that may serve as important genetic modifiers in other organisms, including humans (*25*).

Negative and positive genetic interactions of essential and nonessential genes

The global genetic interaction network, encompassing the majority of both nonessential and essential genes, enabled a comprehensive comparative analysis with other functional information (*8*). Both nonessential and essential genetic interactions were predictive of functionally related gene pairs (Fig. 6, B and C, and fig. S15). In particular, negative interactions among essential genes showed a striking overlap with protein-protein interactions (Fig. 6C and fig. S15). For example, 50% of essential gene pairs whose products physically interact also share a negative interaction, representing a ~10-fold enrichment for protein-protein interactions among essential genes displaying negative genetic interactions. Similarly, 63% of gene pairs annotated to the same essential protein complex were connected by a negative genetic interaction, representing a ~15-fold enrichment for cocomplexed pairs among essential genes connected by negative interactions. In fact, individual negative interactions were as informative as genetic interaction profile similarity for predicting membership to the same essential pathway or complex, a property that does not hold for nonessential genes (fig. S16). This observation highlights the reduced ability of a cell to tolerate multiple partial loss-of-function mutations in the same essential pathway or complex (Fig. 6C and fig. S15).

Consistent with previous observations (*1*), positive genetic interactions between nonessential genes also overlapped with protein-protein interactions, albeit to a lesser extent (0.5%, 3.7-fold enrichment) (Fig. 6C and fig. S15). This reflects that simultaneous perturbation of two genes encoding members of the same nonessential protein complex often shows a fitness defect resembling the corresponding single mutants.

In contrast, we did not detect significant overlap between the positive interactions of essential genes and other molecular or functional relationships, including physical interactions (Fig. 6, B and C, and fig. S15). The lack of a functional signal could not be explained by differences in data quality because replicate analysis confirmed that SGA-derived positive and negative interactions showed similar levels of reproducibility (fig. S2). Furthermore, members of the same essential protein complex or different alleles of the same essential gene often showed similar positive interaction profiles (fig. S17). Thus, while negative interactions identified clear functional relationships between genes, positive interactions among partial loss-of function alleles of essential genes represent a different type of relationship that is not captured by other large-scale data sets or functional standards.

Functional distribution of genetic interactions within and between bioprocesses

We further examined the functional distribution of genetic interactions through the enrichment for negative and positive interactions within and between biological processes (Fig. 1F and data file S6) (*8*). Negative genetic interactions were significantly enriched ($P < 0.05$, hypergeometric) among genes belonging to the same biological process in both the nonessential (NxN) and essential (ExE) genetic interaction networks (Fig. 6D, on-diagonal). Negative interactions were also enriched between deletion alleles of nonessential genes in different biological processes (Fig. 6D, off-diagonal). In contrast, negative interactions between TS alleles of essential genes,

Fig. 6. Negative and positive genetic interactions connecting nonessential and essential genes. (**A**) The network density (observed interactions/total gene pairs screened) of negative (blue) and positive (yellow) genetic interactions, expressed as a fraction of all tested gene pairs, associated with nonessential and essential genes, at a defined threshold (genetic interaction score, $|\varepsilon| > 0.08$, $P < 0.05$). Error bars indicate the standard deviation across multiple samplings of the alleles for essential genes, where each gene is represented by a single, randomly selected allele in each sampling. (**B**) Plots of precision versus recall [number of true positives (TPs)] for negative (blue) and positive (yellow) interactions for nonessential and essential genes, as determined by our genetic interaction score ($|\varepsilon| > 0.08$, $P < 0.05$). TP interactions were defined as those involving gene pairs coannotated to a gold standard set of GO terms. The precision and recall values were calculated as described (*8*). (**C**) Fold enrichment for colocalized, coexpressed, or physically interacting genes among negative (blue) and positive (yellow) genetic interactions connecting pairs of nonessential or essential genes. (**D**) Network density (observed interactions/total gene pairs screened) of genetic interactions within and across biological processes. The fraction of screened nonessential and essential gene pairs exhibiting negative or positive interactions, as determined by our genetic interaction score ($|\varepsilon| > 0.08$, $P < 0.05$), was measured for the 15 gene sets enriched for specific biological processes, as defined in Fig. 1F. Node size reflects the fraction of interacting gene pairs observed for a given pair of biological processes. Dark blue and dark yellow nodes indicate the frequency of interaction that is significantly above random expectation. Light blue and light yellow nodes represent a frequency of interaction that is not significantly higher than random expectation. Nodes on the diagonal represent the frequency of interactions among genes belonging to the same biological process. Nodes off the diagonal represent the frequency of interactions between different biological processes.

despite higher abundance (Fig. 6A), were biased toward gene pairs in the same biological processes (Fig. 6D, on-diagonal) and were rarely enriched between genes involved in different biological processes (Fig. 6D, off-diagonal). Although these trends could reflect the different genetic perturbations used to interrogate nonessential and essential genes, negative interactions among essential genes highlight a core set of cellular bioprocesses, and nonessential genes appear to mediate connections between these bioprocesses.

While nonessential genes involved in the same biological process were modestly enriched for positive interactions, we failed to observe a similar enrichment for positive interactions among functionally related essential genes (Fig. 6D, on-diagonal). Instead, positive interactions tended to connect essential genes with roles in highly distinct biological processes. In particular, we observed significant enrichment for positive interactions that connected essential genes with nuclear-related functions to essential genes required for vesicle traffic–dependent functions (Fig. 6D and fig. S17).

The architecture of negative interactions within the genetic network hierarchy

To explore the functional distribution of genetic interactions in more detail, we examined where genetic interactions occurred within the genetic network hierarchy of gene function derived from profile similarities. Specifically, we assessed how frequently negative interactions connected a pair of genes belonging to the same cluster within the hierarchy of genetic interaction profiles (Fig. 2A), and we examined clusters corresponding to either a cellular compartment, biological process, or pathway/complex (Fig. 7A) (*8*). The density (i.e. the number of observed genetic interactions relative to the total number of gene pairs screened) of negative interactions, among genes in both the nonessential (NxN) and essential (ExE) genetic interaction networks, increased with the functional specificity of a given cluster. Accordingly, genes within a cluster enriched for specific pathways or complexes were connected by negative interactions more often than genes in the same biological process–enriched cluster, which, in turn, were more frequently connected by negative interactions than genes belonging to a cluster enriched for a particular cell compartment (Fig. 7B). For example, essential genes that fall into a cluster within the set that was enriched for complexes/pathways (PCC 0.4 to 0.8) were connected by a negative interaction with a relatively high density (60 to 90%), but they were rarely connected by a

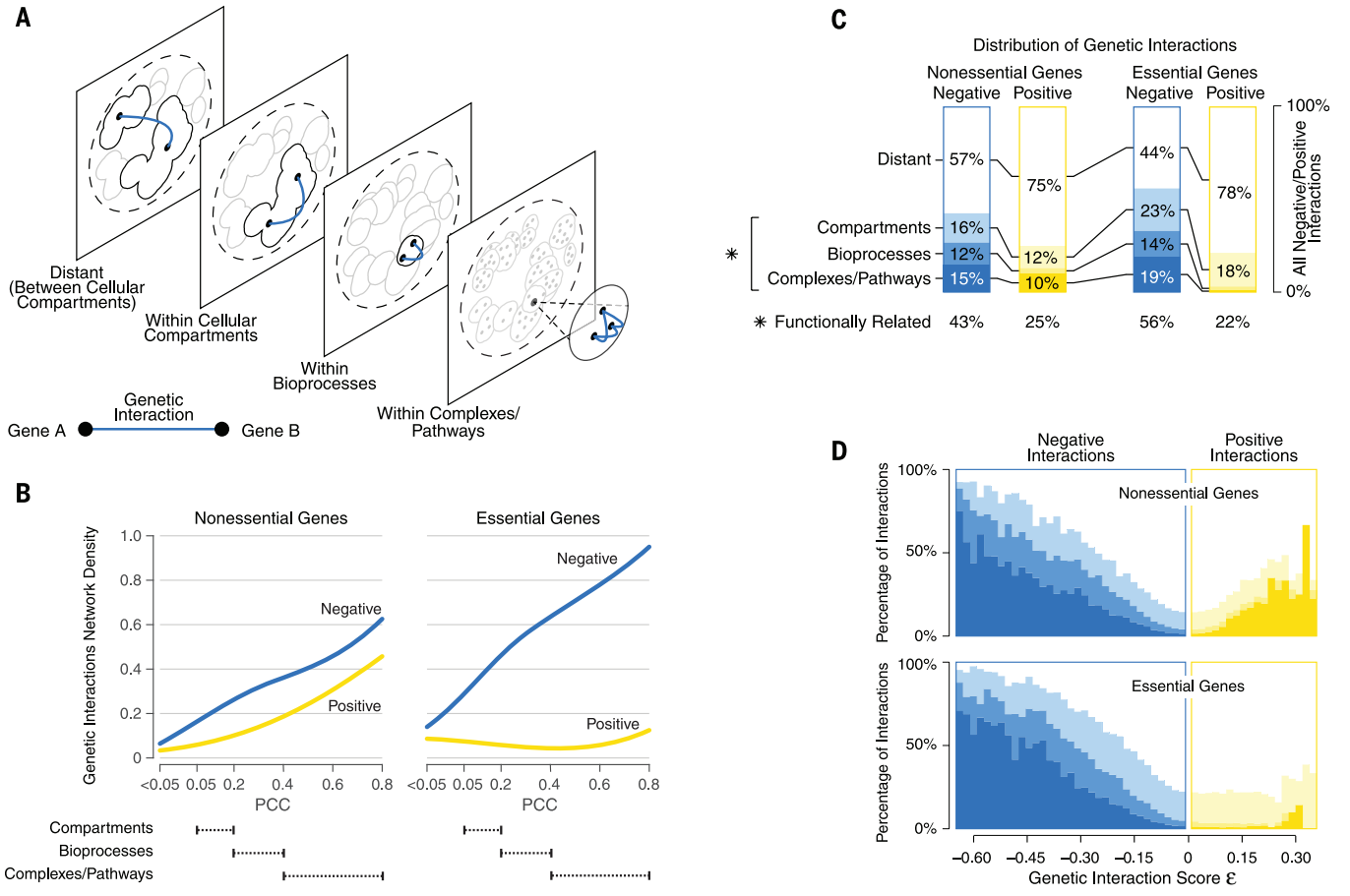

Fig. 7. Mapping negative and positive interactions across the genetic network–based functional hierarchy. (**A**) Schematic representation of the genetic network–based functional hierarchy illustrating interactions between genes within the same complex, biological process, or cellular compartment, as well as distant interactions that span different cellular compartments. (**B**) The network density of genetic interactions between of genes in the same cluster, at a given level of profile similarity (PCC) in the genetic network hierarchy for negative (blue) or positive (yellow) genetic interactions (genetic interaction score, $|\varepsilon| > 0.08$, $P < 0.05$). Dashed lines indicate the PCC range within which clusters in the genetic network hierarchy were enriched for cell compartments, bioprocesses, and protein complexes. (**C**) The functional distribution of all negative (blue) and all positive (yellow) interactions ($|\varepsilon| > 0.08$, $P < 0.05$) among genes in the genetic network hierarchy. The percentage of all interactions connecting nonessential gene pairs and essential gene pairs in the same clusters corresponding to a cell compartment, bioprocess, or complex/pathway is shown. The combined fraction of functionally related interactions (i.e., interactions connecting genes in the same compartment, bioprocess, complex or pathway) is also indicated (*). (**D**) The percentage of negative (blue) and positive (yellow) interactions within a specified genetic interaction score (ε) range that connects genes belonging to the same cluster at the indicated level of the genetic network–based hierarchy. Different shades of blue and yellow correspond to levels of functional relatedness shown in (C). The white area corresponds to the fraction of interactions that connect genes in different cellular compartments (i.e., distant).

positive interaction (Fig. 7B). In total, 43% of nonessential and 56% of essential gene pairs connected by negative interactions shared some degree of functional relatedness (Fig. 7C).

The magnitude of a given negative interaction was also associated with the extent of functional similarity shared between genes (Fig. 7D). For both nonessential and essential genetic interactions, stronger interactions tended to connect genes with closer functional relationships (Fig. 7D). Thus, on the basis of the strength of negative genetic interaction, we can predict whether two genes share an intimate relationship and possibly function in the same pathway or complex. For example, members of the conserved endoplasmic reticulum (ER) membrane protein complex—including *EMC1*, *EMC2*, and *EMC6*, which play a role in phospholipid transfer from the ER to mitochondria to facilitate phosphatidylethanolamine biosynthesis (*26*)—showed strong negative genetic interactions (genetic interaction score < −0.65) with a previously uncharacterized essential gene, *YNL181W*, suggesting a role for this gene in lipid metabolism. Indeed, *YNL181W* encodes a putative oxidoreductase that localizes to the ER (*27*) and, consistent with defective membrane function, *ynl181w* hypomorphic mutants showed altered sensitivities to numerous bioactive compounds (fig. S18) (*8*). We named this gene *PBR1* (potentiates bioactive compound response) to highlight its role in xenobiotic sensitivity.

The architecture of positive interactions within the genetic network hierarchy

Positive interactions among nonessential genes exhibited similar, albeit weaker, trends, where the density of interactions increased gradually with the functional specificity of hierarchy-derived clusters (Fig. 7B) and the magnitude of nonessential positive interactions was predictive of nonessential pathway or complex membership (Fig. 7D). In contrast, the density of positive interactions detected in the essential network was not related to functional specificity. In fact, the most distantly related essential gene pairs were more frequently connected by positive interactions than gene pairs mapping to the same biological process-level clusters (Fig. 7B). The majority of positive interacting gene pairs in both the essential (ExE, 78%) and nonessential (NxN, 75%) genetic interaction networks occurred between distantly connected genes whose products appeared to function in different cell compartments (Fig. 7C). Moreover, we did not observe a relationship between functional similarity and the magnitude of positive interactions between essential gene pairs (Fig. 7D). Thus, positive interactions between essential genes generally appear to reflect more functionally distant relationships.

Genetic interactions within and between protein complexes

Consistent with previous findings (*1*, *5*, *28*, *29*), we found that protein complexes exhibited highly organized patterns of genetic interactions. For example, many protein complexes tested (60 of 141, 43%) were enriched ($P < 0.01$, hypergeometric) for genetic interactions within the set of protein complex–encoding genes and were biased for a single type of interaction, either negative or positive, highlighting the coherent nature of genetic interactions shared among genes encoding members of the same complex. The type of interaction observed within protein complexes depended on essentiality. For example, complexes composed primarily of nonessential genes (>75% nonessential genes) (data file S12) were more often enriched for positive (21%; 20 of 97 complexes) compared with negative (5%; 5 of 97 complexes) interactions among their members (Fig. 8A and data file S13). In contrast, most essential protein complexes (>75% essential genes; data file S12) were enriched for negative interactions among their members (82%; 35 of 44 complexes). Notably, none of the essential complexes in our data set were enriched for positive interactions (Fig. 8A and data file S13).

The genetic interactions occurring within protein complexes can even resolve the structural organization of large, multisubunit complexes. For example, although proteasome genes tend to be connected by negative genetic interactions, genes encoding components of the same subunit (e.g., within 19*S* or within 20*S*) interact more frequently with one another than genes belonging to different subunits (between 19*S* and 20*S*) (fig. S19). Phenotypic differences between proteasome subunits were also supported by chemical-genetic interactions observed in yeast (fig. S19) (*30*), as well as in *Drosophila melanogaster* cultured cells (fig. S20 and data file S14) (*8*), suggesting that the topology of genetic networks connecting genes within protein complexes by uniform sets of genetic interactions is conserved in higher eukaryotes.

We also examined the topology of genetic interactions occurring between protein complexes and found a large number of complex-complex pairs that were both enriched for genetic interactions ($P < 0.001$, hypergeometric) and strongly biased toward either negative or positive interactions (*8*). More complex-complex pairs were connected by coherent sets of negative than positive interactions (Fig. 8B and data file S13). For example, 4% of all nonessential pairs of protein complexes tested (293 of 6899) were connected by negative interactions, whereas positive interactions connected less than 2% of nonessential complexes (130 of 6899). Similarly, 5% (74 of 1597) of all essential complex pairs in our data set were connected by negative interactions, whereas less than 2% (29 of 1597) of essential protein complex pairs shared positive interactions (Fig. 8B and data file S13). Nonetheless, we observed hundreds of instances of both coherent negative (470) and positive (192) interactions connecting pairs of essential and nonessential complexes, emphasizing the highly organized topology of genetic interaction networks (Fig. 8B and data file S13).

Functional wiring diagrams of protein complexes

Extracting all genetic interactions for specific protein complexes generated functional wiring diagrams that revealed the set of genes, pathways, and bioprocesses, modulated by mutation of a particular complex (Fig. 9, A and B). For example, coherent sets of negative interactions involving the ORC, which specifies sites of initiation of DNA replication throughout the genome (*31*), linked functionally related complexes, including the MCM (mini-chromosome maintenance) and the GINS (Go, Ichi, Ni, San) complexes (Fig. 9A), both of which participate in the initiation of DNA replication (*32*, *33*). In another example, negative interactions associated with the 19*S* proteasome highlighted diverse functions that are particularly important when proteasome activity is compromised (Fig. 9B),

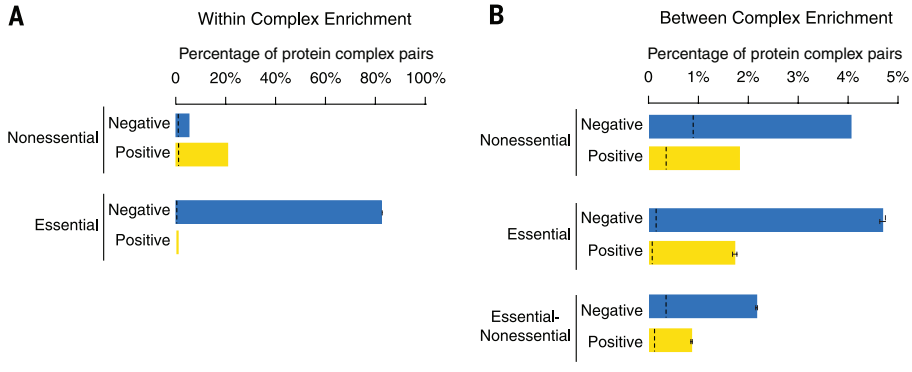

Fig. 8. Genetic interactions within and between protein complexes. (**A**) The percentage of nonessential and essential complexes whose members were enriched for genetic interactions with each other and biased (i.e., coherent) for either mostly negative (blue) or mostly positive (yellow) interactions. (**B**) The percentage of nonessential-nonessential, essential-essential, or essential-nonessential complex-complex pairs found to be enriched for genetic interactions and biased (i.e., coherent) for either mostly negative (blue) or mostly positive (yellow) interactions. Black dashed lines indicate the background rate of coherent genetic interaction enrichment within individual complexes or between pairs of protein complexes. Error bars indicate the standard deviation across multiple samplings of different alleles for the same essential genes, where each gene is represented by a single, randomly selected allele in each sampling.

including interactions with genes encoding the APC (anaphase-promoting complex), which targets cell cycle proteins for degradation to promote exit from mitosis (*34*). Interestingly, essential genes that showed negative interactions with the proteasome were enriched for multidomain proteins, suggesting that TS alleles may perturb folding of more complex proteins, resulting in a greater dependence on proteasome activity in mutants (fig. S21).

Positive interactions among essential genes reflect general regulatory mechanisms

Protein complexes involved in proteostasis, including several chaperones and the proteasome, exhibited among the strongest enrichment for positive genetic interactions, especially in the essential gene network (Fig. 9C, fig. S22, and data file S15). Positive genetic interactions connected the proteasome and other proteostasis-related complexes to genes involved in various functions, including vesicle trafficking and transcription (Figs. 6D and 9B and fig. S23). Because the proteasome plays a direct role in controlling protein turnover, we hypothesized that a subset of its positive interactions may reflect genetic suppression through the stabilization of a mutant protein (*35*). Indeed, we further tested a subset of these positive interactions (*8*) and, based on this analysis, we estimated that ~30% of proteasome-positive interactions represent genetic suppression, where a fitness defect associated with a hypomorphic TS allele of an essential gene is suppressed by a second mutation in a proteasome-encoding gene (table S3, fig. S24, and data file S16). In total, 16% of positive interactions with essential genes appear to be associated with proteostasis. In a similar regulatory relationship, positive interactions were also enriched between genes involved in mRNA decay and essential gene DAmP alleles (*13*), which often affect mRNA stability via disruption of their 3′ untranslated region (fig. S24).

Interestingly, a subset of protein complexes, in addition to being enriched for positive interactions (Fig. 9C), also exhibited more positive interactions compared with negative interactions with essential genes (Fig. 9D and data file S15). The positive interactions of these biased complexes were also more functionally diverse compared with their negative interactions. For example, ORC subunits were connected by coherent sets of positive interactions to genes with roles in several different functions, including members of the ER-associated translocon complex (Fig. 9A). The ORC-translocon connection reflects enrichment for cross-compartment positive interactions observed between genes encoding essential, nuclear, and vesicle traffic-dependent functions (Fig. 6D).

Protein complexes with a positive interaction bias tend to be involved in cell cycle progression, and their disruption often leads to a cell cycle delay or arrest phenotype (Fig. 9D and fig. S22). A cell cycle delay may result when a mutation activates a checkpoint pathway that slows cell cycle progression, allowing the cell to correct an otherwise rate-limiting defect and mask the phenotypic effect normally associated with a second mutation (*36*). Thus, an ORC-dependent S-phase cell cycle delay may mask growth defects associated with perturbation of genes required for polarized secretion during budding, thereby resulting in positive interactions. Protein complexes biased for positive interactions with essential genes also exhibited many negative interactions with checkpoint genes ($P < 4 \times 10^{-56}$; Fisher's exact test) (fig. S22), suggesting that cell viability depends on an active checkpoint response in the absence of these complexes. Genes with cell cycle progression–related roles accounted for 30% of essential gene-positive interactions, which, combined with genes involved in proteostasis, explain 46% of the positive interactions among essential genes.

Discussion

A global network based on genetic interaction profile similarity resolves a hierarchy of modules, enriched for sets of genes within specific pathways and protein complexes, biological processes, or subcellular compartments. In the context of this functional organization, coherent sets of negative and positive genetic interactions connect both within and between the highly resolved complex and pathway modules to map a functional wiring diagram of the cell.

Our comprehensive analysis of genetic interactions among essential genes revealed several illuminating principles. First, consistent with the results of our previous smaller-scale surveys (*1*, *24*), essential genes are major hubs and form the basic scaffold of the global genetic interaction network. Second, the extreme negative or synthetic lethal interactions among essential genes often occur between genes within the same protein complex, or between genes in different protein complexes but within the same biological process or subcellular compartment, properties that may prove useful for predicting genetic interactions in other systems. Third, positive genetic interactions between two essential genes typically do not reflect shared function, but rather often occur between genes in distant cellular compartments and reflect more general regulatory connections associated with a cell cycle delay or proteostasis.

An important property associated with the global network is the potential for digenic interactions to compound the phenotypes associated with single gene mutations. Whereas only ~1000 genes in the yeast genome are individually essential in standard growth conditions and cause lethality when mutated (*9*, *10*), we showed that hundreds of thousands of mutant gene pair combinations result in a negative interaction in the global genetic interaction network, including an extreme set of ~10,000 synthetic lethal interactions between nonessential gene pairs (*8*). In other words, we discovered a genetic background in which an additional ~3300 genes are essential for viability (*8*). Despite the power of this approach for uncovering growth dependencies, ~1000 of the 5400 yeast genes we examined showed relatively few genetic interactions and remain sparsely connected. Our global genetic network was mapped under a particular condition in a specific genetic background, and we anticipate that changing these two key factors may reveal new interactions for many of the sparsely connected genes (*37*). Ultimately, broad mapping of both core and condition-specific genetic interactions promises to accelerate the field of synthetic biology, providing a rational understanding of the requirements for the design of minimal genomes (*38*).

It is also important to consider other types of genetic interactions, beyond those associated with loss-of-function mutations in haploid cells. Our analysis revealed that relatively severe deletion alleles of nonessential genes or TS alleles of essential genes often show extensive digenic interaction profiles. However, it is possible that the more subtle mutations associated with natural genetic variation may require higher-order combinations, involving more than two genes, to modulate phenotype and influence heritability extensively (*39*). One interesting case involves duplicated genes with overlapping function, which often are buffered more extensively, such that more complex triple-mutant analysis will be required to reveal their genetic interaction profiles (*1*, *40*). We must also understand the general principles associated with genetic networks involving gain-of-function alleles and more complex genetic interactions that can occur in diploid and polyploid organisms (*41*), across a variety of different cell types, within whole animals (*42*–*44*), or between hosts and their symbiotic organisms (*45*).

Because negative genetic interactions are highly ordered and often occur as coherent sets, (e.g., predominantly negative genetic interactions connecting genes within a protein complex or between two different protein complexes), many different pairs of mutations may lead to the same terminal synthetic lethal/sick phenotype. We suspect that this network topology is important when considering the genotype-to-phenotype problem in human genetics. Because biological systems are built upon sets of conserved genes whose products participate in functional modules, it is reasonable to expect that the general topology of genetic networks will also be conserved (*25*). As observed for the complex-complex connections on the global yeast genetic network, mutations in many different pairs of genes may lead to the same phenotype, such as a disease state, in humans. This property of genetic networks means that scanning disease cohorts for genetic variation that corresponds to coherent sets of mutations that connect genes within or between protein complexes and pathways (e.g., see functional wiring diagrams for the ORC the 19*S* proteasome in Fig. 9) may reveal genetic networks underlying diseases.

The regulatory mechanisms associated with positive genetic interactions among essential genes, which include genetic suppression interactions, are also potentially relevant to human

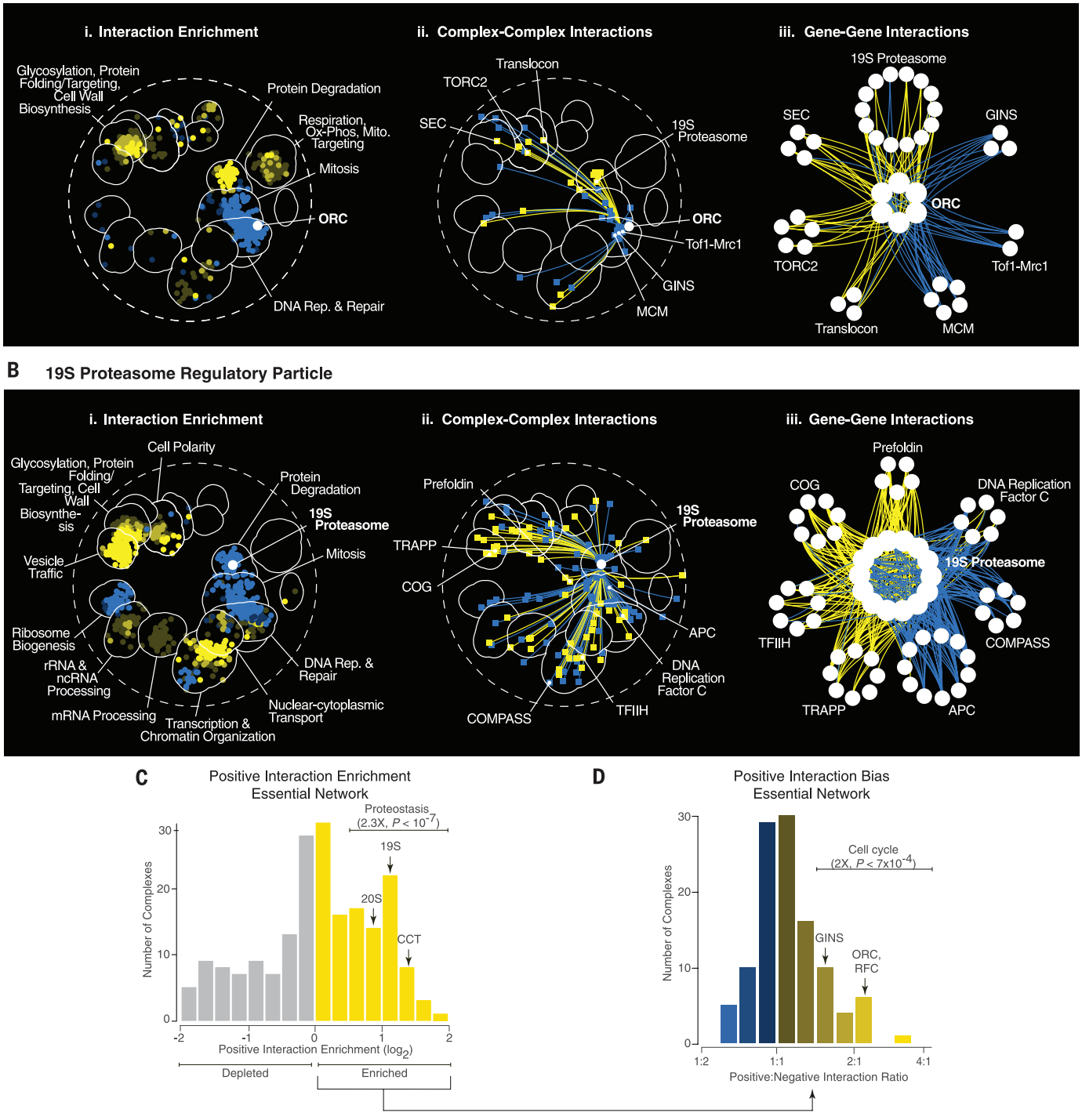

Fig. 9. Functional wiring diagrams for specific protein complexes. (**A**) Genetic interaction map for the ORC. (i) Regions of the global similarity network significantly enriched for genes exhibiting negative (blue) or positive (yellow) genetic interactions with ORC members were mapped using SAFE. (ii) Protein complexes that showed coherent negative or positive genetic interactions with ORC were placed on a schematic representation of the global similarity network based on the average genetic interaction profile similarity of the complex and connected with blue or yellow edges, respectively. (iii) A subset of protein complexes from (ii) that showed coherent negative (blue) or positive (yellow) genetic interactions with genes encoding the ORC are shown. (**B**) Genetic interaction map for the 19S proteasome. The 19S proteasome networks shown in (i) to (iii) were constructed as described in (A). (**C**) Distribution of positive genetic interaction enrichment for protein complexes screened against the essential gene array (TSA). Protein complexes enriched for positive interactions with essential genes (yellow bars) tend to be associated with proteostasis-related functions (2.3X, $P < 10^{-7}$; Fisher's exact test), including the 19S and 20S proteasome subunits as well as the chaperonin-containing T complex (CCT) and prefoldin chaperone complexes (indicated on the graph). (**D**) Distribution of positive versus negative genetic interactions for protein complexes enriched for positive interactions shown in (C). Essential protein complexes that show a bias toward positive interactions, such as the ORC, RFC, and GINS, are often required for normal cell cycle progression (2X, $P < 7 \times 10^{-4}$; Fisher's exact test).

genetics because they may inspire therapeutic approaches and elucidate mechanisms of heritability (*46*, *47*). Notably, mutations that compromise the cellular proteostasis network often suppressed TS alleles of essential genes (table S3 and data file S16). It is possible that, similar to yeast, certain variants of the human proteasome also suppress the detrimental effects of genetic variation associated with numerous other genes, and their corresponding complexes and pathways, within the human genome. Although the genes encoding the proteasome are essential in human cells, and severe mutations in these genes may cause disease (*48*), genetic variation that modulates proteasome function subtly may have the potential to be disease protective.

It is clear that the digenic interactions we have mapped in yeast can be conserved in different yeast species over hundreds of millions of years of evolution (*49*, *50*). Likewise, conservation of genetic interactions from yeast to human cells has been observed (*51*, *52*), particularly within fundamental bioprocesses like DNA synthesis and repair and chromosome segregation, which is particularly relevant for the identification of targets for novel synthetic lethal cancer therapies (*53*, *54*). However, the general extent and breadth of network conservation remain largely unexplored. Importantly, genome-scale application of CRISPR (clustered regularly interspaced short palindromic repeats)–Cas9 genome editing approaches offer the potential to map global genetic interaction networks in human cells (*55*–*57*). We suspect that the general principles of the global yeast genetic network described here will be highly relevant for both the efficient mapping and the interpretation of analogous networks in a variety of different cells and organisms.

Methods summary

Methods for construction of yeast double-mutant strains, identification, and measurement of genetic interactions—as well as all analyses pertaining to genetic interaction profiles and negative and positive interactions—are described in detail in the supplementary materials. General information about our methods, accompanied by specific references to the supplementary materials, is included throughout the text.

REFERENCES AND NOTES

1. M. Costanzo *et al*., The genetic landscape of a cell. *Science* **327**, 425–431 (2010). doi: 10.1126/science.1180823; pmid: 20093466
2. J. L. Hartman 4th, B. Garvik, L. Hartwell, Principles for the buffering of genetic variation. *Science* **291**, 1001–1004 (2001). doi: 10.1126/science.291.5506.1001; pmid: 11232561
3. O. Zuk, E. Hechter, S. R. Sunyaev, E. S. Lander, The mystery of missing heritability: Genetic interactions create phantom heritability. *Proc. Natl. Acad. Sci. U.S.A.* **109**, 1193–1198 (2012). doi: 10.1073/pnas.1119675109; pmid: 22223662
4. J. S. Bloom *et al*., Genetic interactions contribute less than additive effects to quantitative trait variation in yeast. *Nat. Commun.* **6**, 8712 (2015). doi: 10.1038/ncomms9712; pmid: 26537231
5. A. Baryshnikova *et al*., Quantitative analysis of fitness and genetic interactions in yeast on a genome scale. *Nat. Methods* **7**, 1017–1024 (2010). doi: 10.1038/nmeth.1534; pmid: 21076421
6. T. Roemer, C. Boone, Systems-level antimicrobial drug and drug synergy discovery. *Nat. Chem. Biol.* **9**, 222–231 (2013). doi: 10.1038/nchembio.1205; pmid: 23508188
7. H. E. Bryant *et al*., Specific killing of BRCA2-deficient tumours with inhibitors of poly(ADP-ribose) polymerase. *Nature* **434**, 913–917 (2005). doi: 10.1038/nature03443; pmid: 15829966
8. Materials and methods are available as supporting materials on *Science* Online.
9. E. A. Winzeler *et al*., Functional characterization of the *S. cerevisiae* genome by gene deletion and parallel analysis. *Science* **285**, 901–906 (1999). doi: 10.1126/science.285.5429.901; pmid: 10436161
10. G. Giaever *et al*., Functional profiling of the *Saccharomyces cerevisiae* genome. *Nature* **418**, 387–391 (2002). doi: 10.1038/nature00935; pmid: 12140549
11. M. Kofoed *et al*., An updated collection of sequence barcoded temperature-sensitive alleles of yeast essential genes. *Genes Genomes Genetics* **5**, 1879–1887 (2015). doi: 10.1534/g3.115.019174; pmid: 26175450
12. Z. Li *et al*., Systematic exploration of essential yeast gene function with temperature-sensitive mutants. *Nat. Biotechnol.* **29**, 361–367 (2011). doi: 10.1038/nbt.1832; pmid: 21441928
13. M. Schuldiner *et al*., Exploration of the function and organization of the yeast early secretory pathway through an epistatic miniarray profile. *Cell* **123**, 507–519 (2005). doi: 10.1016/j.cell.2005.08.031; pmid: 16269340
14. M. Ashburner *et al*., Gene ontology: Tool for the unification of biology. *Nat. Genet.* **25**, 25–29 (2000). doi: 10.1038/75556; pmid: 10802651
15. A. Baryshnikova, Systematic functional annotation and visualization of biological networks. *Cell Syst.* **2**, 412–421 (2016).
16. J. Dutkowski *et al*., A gene ontology inferred from molecular networks. *Nat. Biotechnol.* **31**, 38–45 (2013). doi: 10.1038/nbt.2463; pmid: 23242164
17. J. L. Koh *et al*., CYCLoPs: A comprehensive database constructed from automated analysis of protein abundance and subcellular localization patterns in *Saccharomyces cerevisiae*. *Genes Genomes Genetics* **5**, 1223–1232 (2015). doi: 10.1534/g3.115.017830; pmid: 26048563
18. T. A. Sangster, S. Lindquist, C. Queitsch, Under cover: Causes, effects and implications of Hsp90-mediated genetic capacitance. *BioEssays* **26**, 348–362 (2004). doi: 10.1002/bies.20020; pmid: 15057933
19. S. Chan, E. A. Choi, Y. Shi, Pre-mRNA 3′-end processing complex assembly and function. *RNA* **2**, 321–335 (2011). doi: 10.1002/wrna.54; pmid: 21957020
20. J. M. Gordon *et al*., Reconstitution of CF IA from overexpressed subunits reveals stoichiometry and provides insights into molecular topology. *Biochemistry* **50**, 10203–10214 (2011). doi: 10.1021/bi200964p; pmid: 22026644
21. F. Abe, H. Minegishi, Global screening of genes essential for growth in high-pressure and cold environments: Searching for basic adaptive strategies using a yeast deletion library. *Genetics* **178**, 851–872 (2008). doi: 10.1534/genetics.107.083063; pmid: 18245339
22. S. G. Addinall *et al*., A genomewide suppressor and enhancer analysis of cdc13-1 reveals varied cellular processes influencing telomere capping in *Saccharomyces cerevisiae*. *Genetics* **180**, 2251–2266 (2008). doi: 10.1534/genetics.108.092577; pmid: 18845848
23. A. Greenall *et al*., A genome wide analysis of the response to uncapped telomeres in budding yeast reveals a novel role for the NAD^+ biosynthetic gene BNA2 in chromosome end protection. *Genome Biol.* **9**, R146 (2008). doi: 10.1186/gb-2008-9-10-r146; pmid: 18828915
24. S. Mnaimneh *et al*., Exploration of essential gene functions via titratable promoter alleles. *Cell* **118**, 31–44 (2004). doi: 10.1016/j.cell.2004.06.013; pmid: 15242642
25. E. N. Koch *et al*., Conserved rules govern genetic interaction degree across species. *Genome Biol.* **13**, R57 (2012). doi: 10.1186/gb-2012-13-7-r57; pmid: 22747640
26. S. Lahiri *et al*., A conserved endoplasmic reticulum membrane protein complex (EMC) facilitates phospholipid transfer from the ER to mitochondria. *PLOS Biol.* **12**, e1001969 (2014). doi: 10.1371/journal.pbio.1001969; pmid: 25313861
27. R. Sánchez, A. Sali, Large-scale protein structure modeling of the *Saccharomyces cerevisiae* genome. *Proc. Natl. Acad. Sci. U.S.A.* **95**, 13597–13602 (1998). doi: 10.1073/pnas.95.23.13597; pmid: 9811845
28. D. Segrè, A. Deluna, G. M. Church, R. Kishony, Modular epistasis in yeast metabolism. *Nat. Genet.* **37**, 77–83 (2005). pmid: 15592468
29. S. Bandyopadhyay, R. Kelley, N. J. Krogan, T. Ideker, Functional maps of protein complexes from quantitative genetic interaction data. *PLOS Comput. Biol.* **4**, e1000065 (2008). doi: 10.1371/journal.pcbi.1000065; pmid: 18421374
30. D. Hoepfner *et al*., High-resolution chemical dissection of a model eukaryote reveals targets, pathways and gene functions. *Microbiol. Res.* **169**, 107–120 (2014). doi: 10.1016/j.micres.2013.11.004; pmid: 24360837
31. S. P. Bell, The origin recognition complex: From simple origins to complex functions. *Genes Dev.* **16**, 659–672 (2002). doi: 10.1101/gad.969602; pmid: 11914271
32. M. Lei, B. K. Tye, Initiating DNA synthesis: From recruiting to activating the MCM complex. *J. Cell Sci.* **114**, 1447–1454 (2001). pmid: 11282021
33. S. A. MacNeill, Structure and function of the GINS complex, a key component of the eukaryotic replisome. *Biochem. J.* **425**, 489–500 (2010). doi: 10.1042/BJ20091531; pmid: 20070258
34. J. M. Peters, The anaphase promoting complex/cyclosome: A machine designed to destroy. *Nat. Rev. Mol. Cell Biol.* **7**, 644–656 (2006). doi: 10.1038/nrm1988; pmid: 16896351
35. F. Khosrow-Khavar *et al*., The yeast ubr1 ubiquitin ligase participates in a prominent pathway that targets cytosolic thermosensitive mutants for degradation. *Genes Genomes Genetics* **2**, 619–628 (2012). doi: 10.1534/g3.111.001933; pmid: 22670231
36. R. Li, A. W. Murray, Feedback control of mitosis in budding yeast. *Cell* **66**, 519–531 (1991). doi: 10.1016/0092-8674(81)90015-5; pmid: 1651172
37. S. Bandyopadhyay *et al*., Rewiring of genetic networks in response to DNA damage. *Science* **330**, 1385–1389 (2010). doi: 10.1126/science.1195618; pmid: 21127252
38. C. A. Hutchison 3rd *et al*., Design and synthesis of a minimal bacterial genome. *Science* **351**, aad6253 (2016). doi: 10.1126/science.aad6253; pmid: 27013737
39. R. D. Dowell *et al*., Genotype to phenotype: A complex problem. *Science* **328**, 469 (2010). doi: 10.1126/science.1189015; pmid: 20413493
40. B. VanderSluis *et al*., Genetic interactions reveal the evolutionary trajectories of duplicate genes. *Mol. Syst. Biol.* **6**, 429 (2010). doi: 10.1038/msb.2010.82; pmid: 21081923
41. D. Altshuler, M. J. Daly, E. S. Lander, Genetic mapping in human disease. *Science* **322**, 881–888 (2008). doi: 10.1126/science.1156409; pmid: 18988837
42. B. Lehner, C. Crombie, J. Tischler, A. Fortunato, A. G. Fraser, Systematic mapping of genetic interactions in *Caenorhabditis elegans* identifies common modifiers of diverse signaling pathways. *Nat. Genet.* **38**, 896–903 (2006). doi: 10.1038/ng1844; pmid: 16845399
43. A. B. Byrne *et al*., A global analysis of genetic interactions in *Caenorhabditis elegans*. *J. Biol.* **6**, 8 (2007). doi: 10.1186/jbiol58; pmid: 17897480
44. B. Fischer *et al*., A map of directional genetic interactions in a metazoan cell. *eLife* **4**, e05464 (2015). doi: 10.7554/eLife.05464; pmid: 25748138
45. R. Blekhman *et al*., Host genetic variation impacts microbiome composition across human body sites. *Genome Biol.* **16**, 191 (2015). doi: 10.1186/s13059-015-0759-1; pmid: 26374288
46. C. M. Buchovecky *et al*., A suppressor screen in Mecp2 mutant mice implicates cholesterol metabolism in Rett syndrome. *Nat. Genet.* **45**, 1013–1020 (2013). doi: 10.1038/ng.2714; pmid: 23892605
47. K. M. Keeling, X. Xue, G. Gunn, D. M. Bedwell, Therapeutics based on stop codon readthrough. *Annu. Rev. Genomics Hum. Genet.* **15**, 371–394 (2014). doi: 10.1146/annurev-genom-091212-153527; pmid: 24773318
48. P. Tsvetkov *et al*., Compromising the 19S proteasome complex protects cells from reduced flux through the proteasome. *eLife* **4**, e08467 (2015). doi: 10.7554/eLife.08467; pmid: 26327695
49. S. J. Dixon *et al*., Significant conservation of synthetic lethal genetic interaction networks between distantly related eukaryotes. *Proc. Natl. Acad. Sci. U.S.A.* **105**, 16653–16658 (2008). doi: 10.1073/pnas.0806261105; pmid: 18931302
50. A. Roguev *et al*., Conservation and rewiring of functional modules revealed by an epistasis map in fission yeast. *Science* **322**, 405–410 (2008). doi: 10.1126/science.1162609; pmid: 18818364
51. R. Deshpande *et al*., A comparative genomic approach for identifying synthetic lethal interactions in human cancer. *Cancer Res.* **73**, 6128–6136 (2013). doi: 10.1158/0008-5472.CAN-12-3956; pmid: 23980094
52. K. J. McManus, I. J. Barrett, Y. Nouhi, P. Hieter, Specific synthetic lethal killing of RAD54B-deficient human colorectal cancer cells by FEN1 silencing. *Proc. Natl. Acad. Sci. U.S.A.* **106**, 3276–3281 (2009). doi: 10.1073/pnas.0813414106; pmid: 19218431
53. D. M. van Pel *et al*., An evolutionarily conserved synthetic lethal interaction network identifies FEN1 as a broad-spectrum

target for anticancer therapeutic development. *PLOS Genet.* **9**, e1003254 (2013). doi: 10.1371/journal.pgen.1003254; pmid: 23382697
54. L. H. Hartwell, P. Szankasi, C. J. Roberts, A. W. Murray, S. H. Friend, Integrating genetic approaches into the discovery of anticancer drugs. *Science* **278**, 1064–1068 (1997). doi: 10.1126/science.278.5340.1064; pmid: 9353181
55. T. Hart *et al.*, High-resolution CRISPR screens reveal fitness genes and genotype-specific cancer liabilities. *Cell* **163**, 1515–1526 (2015). doi: 10.1016/j.cell.2015.11.015; pmid: 26627737
56. T. Wang *et al.*, Identification and characterization of essential genes in the human genome. *Science* **350**, 1096–1101 (2015). doi: 10.1126/science.aac7041; pmid: 26472758
57. V. A. Blomen *et al.*, Gene essentiality and synthetic lethality in haploid human cells. *Science* **350**, 1092–1096 (2015). doi: 10.1126/science.aac7557; pmid: 26472760

ACKNOWLEDGMENTS

We thank D. Botstein, H. Bussey, A. Fraser, H. Friesen, M. Meneghini, and M. Tyers for critical comments. This work was primarily supported by the National Institutes of Health (R01HG005853) (C.B., B.A., and C.L.M.), Canadian Institutes of Health Research (FDN-143264 and FDN-143265) (C.B. and B.A.), RIKEN Strategic Programs for R&D (C.B.), JSPS Kakenhi (15H04483) (C.B.), National Institutes of Health (R01HG005084 and R01GM104975) (C.L.M), and the National Science Foundation (DBI\0953881) (C.L.M.). Computing resources and data storage services were partially provided by the Minnesota Supercomputing Institute and the UMN Office of Information Technology, respectively. Additional support was provided by the Canadian Institutes of Health Research (A.A.C.), National Science Foundation (MCB\1244043) (C.M.), European Research Council (ERC) Advanced Investigator Grant (AdG-294542) (L.M.S), ERC Advanced Grant (European Commission) (M.B.), Ministry of Education, Culture, Sports, Sciences and Technology, MEXT (15H04402) (Y.O.), Canadian Institutes of Health Research (FDN143301), Genome Canada Genome Innovation network (through the Ontario Genomics Institute) (A.-C.G), the Ontario Genomics Institute, Canadian Cystic Fibrosis Foundation, Canadian Cancer Society, Pancreatic Cancer Canada, University Health Network (I.S.), National Science Foundation, Cyber-Enabled Discover and Innovation (CDI) (OIA-1028394), ERC Starting Independent Researcher Grant (278212), ARRS project (J1-5424), Serbian Ministry of Education and Science Project 11144006 (N.P.), National Natural Science Foundation of China (T.X), RIKEN Foreign Postdoctoral Researcher Program (J.S.P., S.C.L.), National Science Foundation Graduate Research Fellowship (NSF 00039202) (E.N.K. and S.W.S), U. of Minnesota Doctoral Dissertation Fellowship (B.V. and E.N.K.). O.G.T, C.L.M, B.A., and C.B are fellows of the Canadian Institute for Advanced Research (CIFAR). All data files (Data Files S1 to 17) associated with this study are described in detail in the supplementary materials and can be downloaded from http://boonelab.ccbr.utoronto.ca/supplement/costanzo2016. Data Files S1 to S17 were also deposited in the DRYAD Digital Repository (doi:10.5061/dryad.4291s). Raw mass spectrometry data and downloadable identification and SAINTexpress results tables were deposited in the MassIVE repository housed at the Center for Computational Mass Spectrometry at UCSD (http://proteomics.ucsd.edu/ProteoSAFe/datasets.jsp). The endogenously tagged GFP and Gal-inducible hemagglutinin data sets have been assigned the MassIVE IDs MSV000079157 and MSV000079368 and are available for FTP download at ftp://MSV000079157@massive.ucsd.edu and ftp://MSV000079368@massive.ucsd.edu, respectively. The data sets were assigned the ProteomeXchange Consortium (http://proteomecentral.proteomexchange.org) identifiers PXD002368 and PXD003147 (data set password: SGA).

SUPPLEMENTARY MATERIALS

www.sciencemag.org/content/353/6306/aaf1420/suppl/DC1
Materials and Methods
Figs. S1 to S24
Tables S1 to S3
Data File Descriptions
References (*58*–*120*)

10.1126/science.aaf1420

A global genetic interaction network maps a wiring diagram of cellular function

Michael Costanzo, Benjamin VanderSluis, Elizabeth N. Koch, Anastasia Baryshnikova, Carles Pons, Guihong Tan, Wen Wang, Matej Usaj, Julia Hanchard, Susan D. Lee, Vicent Pelechano, Erin B. Styles, Maximilian Billmann, Jolanda van Leeuwen, Nydia van Dyk, Zhen-Yuan Lin, Elena Kuzmin, Justin Nelson, Jeff S. Piotrowski, Tharan Srikumar, Sondra Bahr, Yiqun Chen, Raamesh Deshpande, Christoph F. Kurat, Sheena C. Li, Zhijian Li, Mojca Mattiazzi Usaj, Hiroki Okada, Natasha Pascoe, Bryan-Joseph San Luis, Sara Sharifpoor, Emira Shuteriqi, Scott W. Simpkins, Jamie Snider, Harsha Garadi Suresh, Yizhao Tan, Hongwei Zhu, Noel Malod-Dognin, Vuk Janjic, Natasa Przulj, Olga G. Troyanskaya, Igor Stagljar, Tian Xia, Yoshikazu Ohya, Anne-Claude Gingras, Brian Raught, Michael Boutros, Lars M. Steinmetz, Claire L. Moore, Adam P. Rosebrock, Amy A. Caudy, Chad L. Myers, Brenda Andrews and Charles Boone (September 22, 2016)
Science **353** (6306), . [doi: 10.1126/science.aaf1420]

Editor's Summary

Science (print ISSN 0036-8075; online ISSN 1095-9203) is published weekly, except the last week in December, by the American Association for the Advancement of Science, 1200 New York Avenue NW, Washington, DC 20005.